SESSION 4: MINE-SLOPE STABILITY

Page No.

Application and Analysis of Anchored Geosynthetic Systems for Stabilization of Abandoned Mine Land Slopes.
Stanley J. Vitton, M. Frank Whitman, Wendell Harris, Robert Y. Liang 256

Maximum Safe Slope Angles for Proposed Shiplock Slopes of Three Gorges Dam Site Based on Kinematic Analyses Performed on Major Discontinuities.
Jeong-gi Um, Pinnaduwa H.S.W. Kulatilake, Jianping Chen, Jianren Teng 267

Application of Soil Nails to the Stability of Mine Waste Slopes.
Clyde R. Tant, Eric C. Drumm, Matthew Mauldon, Richard M. Berry 282

AMERICAN SOCIETY • SURFACE MINING and RECLAMATION •

APPLICATION AND ANALYSIS OF ANCHORED GEOSYNTHETIC SYSTEMS FOR STABILIZATION OF ABANDONED MINE LAND SLOPES

by

Stanley J. Vitton, M. Frank Whitman, Wendell W. Harris, and Robert Y. Liang

Abstract. An anchored geosynthetic system (AGS) was used in the remediation of a landslide associated with an abandoned coal mine located near Hindman, Kentucky. In concept, AGS is a system that provides in-situ stabilization of soil slopes by combining a surface-deployed geosynthetic with an anchoring system of driven reinforcing rods similar to soil nailing. Installation of the system involves tensioning a geosynthetic over a slope's surface by driving anchors through the geosynthetic at a given spacing and distance. By tensioning the geosynthetic over the slope's surface, a compressive load is applied to the slope. Benefits of AGS are described to include the following: (1) increase soil strength due to soil compression including increased compressive loading on potential failure surfaces, (2) soil reinforcement through soil nailing, (3) halt of soil creep, (4) erosion control, and (5) long term soil consolidation. Following installation of the AGS and one year of monitoring, it was found that the anchored geosynthetic system only provided some of the reported benefits and in general did not function as an active stabilization system. This was due in part to the inability of the system to provide and maintain loading on the geosynthetic. The geosynthetic, however, did tension when slope movement occurred and prevented the slope from failing. Thus, the system functioned more as a passive restraint system and appeared to function well over the monitoring period.

Additional Key Words: slope stability, landslide remediation, geotextiles.

Introduction

A significant problem in abandoned mine lands is the stabilization of unstable slopes. According to Iannacchione et al., (1994), the Abandoned Mine Lands program, administered by the Office of Surface Mining (OSM), has spent approximately $64 million remediating 425 landslides between 1979 and 1992, at an average cost of $152,000 per landslide. In Kentucky alone, $45 million was spent during this period on 268 landslides.

In an attempt to reduce the cost of landslide remediation as well as to provide more efficient alternatives for landslide remediation, several new systems have been considered. One of the systems considered is an anchored geosynthetic system (AGS), which was proposed by Koerner (1984, 1985, 1986a) and Koerner and Robbins (1986c) in the mid-1980s. To evaluate this system an AGS was installed and monitored on a landslide associated with an abandoned mine site near Hindman located in Eastern Kentucky (Figure 1).

The basic function of an AGS is to provide active stabilization of the slope through tensioning a geosynthetic over a slope using ground anchors as illustrated in Figure 2. As the soil beneath the

---

[1]Paper presented at the 13th Annual National Meeting American Society for Surface Mining and Reclamation, Knoxville, Tennessee, May 18 to 23, 1996.

[2]Stanley J. Viiton is Assistant Professor of Civil & Environmental Engineering, Michigan Technoloical University, Houghton, MI 49931; M. Frank Whitman is an Engineer, Testing Incorporated, Decatur, AL 35602; Wendell W. Harris is Assistant Professor of Civil & Environmnetal Engineering, University of Alabama, 35487; Robert Y. Liang is Professor & Head of Civil & Environmental Engineering, University of Akron, OH 44325.

[3]Publication in this proceedings does not prevent the authors from publishing their manuscripts, whole or in part, in other publication outlets.

geosynthetic deforms, membrane stresses develop in the tensioned geosynthetic and impart a compressive load onto the slope, which increases the stability of the slope. According to Koerner, anchorage of the geosynthetic is achieved with small diameter, ribbed steel rods (rebar) that are driven into the soil using hand held tools such as a vibropercussion hammer. The anchors are driven on a prescribed grid pattern through the geosynthetic, generally at right angles to the ground surface, to approximately 75 to 90% of their designed depth. The geosynthetic is then fastened to the anchor and the anchor is driven the remaining distance, thereby tensioning the geosynthetic and creating a curved geosynthetic-soil interface as the soil deforms the soil below the geosynthetic. This tension and curvature imparts compressive stress to the soil and an uplift loading on the anchor. According to Vitton (1991), this compressive stress, σ_{nr}, which is applied to the soil from the geosynthetic through membrane action, is directly related to the tension, N, in the geosynthetic (developed by the driving force of the anchor) and inversely related to the radius of curvature, r_c, of the geosynthetic-soil interface (from the deformation of the soil beneath the geosynthetic) as follows

$$\sigma_{nr} = \frac{N}{r_c} \qquad (1)$$

Koerner (1986a) lists the immediate and long term benefits of utilizing AGS for slope stabilization as follows:

1. Immediate slope stabilization due to bending and shearing resistance of the anchors.
2. Immediate halt to long term slope creep.
3. Immediate stabilization of the potential failure zone due to an increase in compressive stresses on the potential failure plane.
4. Immediate erosion control of the slope surface.
5. Increasing slope stability in the long term due to consolidation of cohesive soils and the densification of cohesionless soils from the compressive loading on the soil.

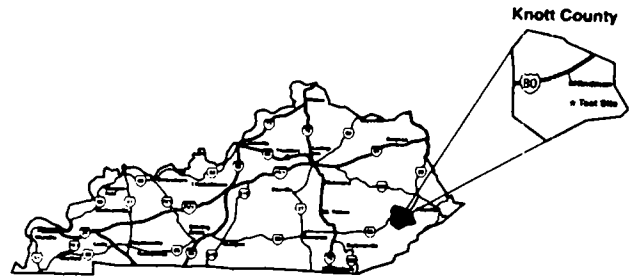

Figure 1. AGS project site location map.

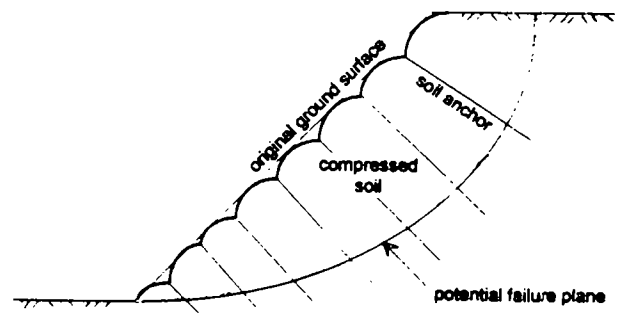

Figure 2. Cross-section of an anchored geosynthetic system.

However, as noted by Koerner, the system may require additional anchor redriving after the initial installation to maintain tension in the geosynthetic due to soil consolidation and stress relaxation in the geosynthetic. In addition to these benefits, AGS also eliminates the need for heavy construction equipment to repair the slope, resulting in substantial cost savings.

To date, only limited field research has been conducted on AGS. As previously stated, the original design concept was developed by Koerner (1984, 1985), who also performed the first theoretical AGS slope stability analysis (Koerner and Robins, 1986). Other theoretical work was done by Hryciw (1991, 1992), who calculated the optimum length and orientation of soil anchors in cohesionless soils, and by Greenwood (1985), who analyzed a soft clay slope that was remediated with a geogrid connected to duck-billed anchors.

Two field installations were completed by Koerner (1986) using a woven slit-film geotextile. This fabric was fitted with grommets on a 1.5 m (5 ft) triangular pattern and anchored to the slope using 13 mm (0.5 in) diameter steel rods. These rods were 1.2 m (4 ft) long and were coupled together to create total anchor lengths of 1.2 m (4 ft) to 7.3 m (24 ft). These lengths were varied so as to penetrate the potential failure plane by at least a meter. This design was used to stabilize a 10.7 m (35 ft) high, 60° slope of silty sand and a 4.5 m (15 ft) high, 50° slope of silty clay. Both slopes remained stable for one year, but no information has yet been published on the long-term effects of the installations.

Vitton's (1991) research, however, revealed that for cohesionless soil, the deformation of the geosynthetic-soil interface is limited to an area immediately around each anchor. This and the development of interface frictional forces on the geosynthetic limit the compressive load that can be applied to the slope. Vitton also noted that stress relaxation of the geosynthetic limits the amount of time that the system is in tension.

Research Site

The research site selected is located in Eastern Kentucky and is approximately 1.5 km south of Hindman, Kentucky in Knott County as shown in Figure 1. The landslide lies approximately 230 m (750 ft) downslope from the Fire Clay (Hazard Number Four) coal bed, which was mined in the early 1970's. A 3 ha (7 acre) landslide occurred in the mine spoil in May of 1984, sliding downslope approximately 275 meters (1000 ft) into the center of a hollow and onto a county road at the base of the hollow. The failure was remediated by the Kentucky Office of Surface Mining (OSM) as an Abandoned Mine Land (AML) project called the Madden Slide. Due to the volume of the spoil, some of it was kept at the site in an uncompacted head-of-hollow fill. In constructing the fill, part of an adjacent slope, which had not been disturbed by the original landslide, was cut back to allow for a drainage ditch to be constructed around the head-of-hollow fill. The undercut slope eventually failed in 1988 and was remediated in 1991. The slide failed again in 1993. The main cause of the instability was groundwater seepage, which was observed in at least three locations within the landslide. Due to the nature of this slide and size of the adjacent landslide, this landslide was selected for the installation and evaluation of the AGS. A cross-section of the slide is shown in Figure 3 while a plan view of the landslide area is shown in Figure 4.

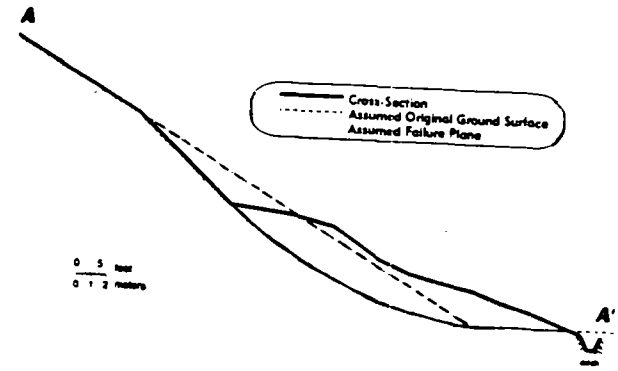

Figure 3. Cross-section of the landslide prior to remediation.

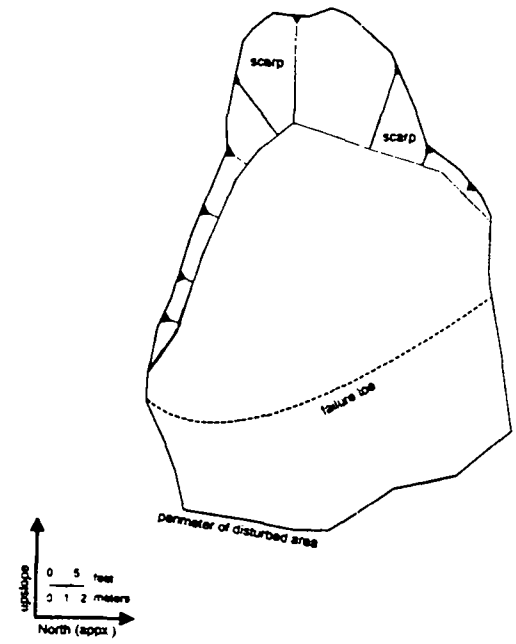

Figure 4. Plan view of landslide area.

The slope in which the slide occurred consists of colluvial soils formed from the overlying rock formations and containing significant sandstone fragments. The USCS classification for

the soil is ML, a sandy silt. However, the Atterberg limits did plot very close to the hatched zone of the plasticity chart indicating a silt-clay mixture. The liquid limit was found to vary between 25 and 35 with an average value of approximately 28. The plastic limit varied between 17 and 25 with an average value of approximately 22. The corresponding plasticity index was approximately 6, indicating a material of low plasticity. As expected the moisture content of the surface soils varied by season. Average moisture contents in the spring were typically around 30%, while in the fall the moisture content decreased to an average value of 16%. These water content values indicate a liquidity index of greater than one during the spring and less than zero during the fall. The softer response in the spring coincides with the increase of water content when a slope failure occurred.

Consolidation tests were conducted since soil consolidation will result when the compressive load from the geotextile is applied to the slope's surface. It was found that the coefficient of consolidation, c_v, averaged 15 m^2/yr while the virgin compression index, C_c, averaged 0.132 and the recompression index averaged 0.025. The preconsolidation pressure, which was difficult to determine, was estimated to be approximately 100 kPa (2100 psf) for soil samples from an undisturbed area adjacent to the slide at a depth of 0.6 m (2 ft). This indicates that the colluvial soils were overconsolidated. Although the past maximum pressure is given with some reservation due primarily to the disturbance during sampling, it does indicate that the soils are overconsolidated probably due to the wetting and drying cycles that develop the desiccated crust.

To estimate the shear strength of the colluvial soil, a series of consolidated-undrained shearing triaxial compression tests and unconsolidated-undrained compression tests were performed on shelby tube samples taken from the site. The drained strength parameters were found to be as follows; the effective angle of internal friction, ϕ', was approximately 33°, while the effective cohesion, c', was approximately 3.5 kPa. The undrained shear strength, S_u, was approximately 23 kPa (1100 psf). This would indicate a soil of medium consistency. However, the undrained shear strength would be expected to be significantly less during the wetter spring months when the natural water content was higher.

System Design and Installation

The general design of the AGS installed followed the original system proposed by Koerner (1984) with modifications as suggested by Vitton (1991). The as-constructed system, however, was based primarily on site conditions and dimensions and on anchor driving tests. Unexpected developments in the field and accumulated experience necessitated changes in the original AGS design during actual installation. Due to delays, the installation of the system was completed over a period of four months, although the total installation time was only approximately two and half weeks using an average of four people. The components of the AGS consisted of (1) geotextile, (2) anchors, and (3) a geotextile-anchor connection. The following section provides the selection and design of each these components and the installation procedure used for the AGS.

Geotextile

Since a high to moderate strength geotextile is required for an AGS, only woven geotextiles were considered for this project. Other fabric properties of concern were stress relaxation, ultraviolet (UV) radiation stability, fabric construction, and stress-strain characteristics. The fabric selected for installation was Linq's (formally Exxon) GTF-1000T, a woven polyester geotextile. This fabric has a tensile strength of 160 kN/m (925 lb/in) in the warp direction and 140 kN/m (800 lb/in) in the fill direction. The fabric strength selected was based on the pullout resistances of the ground anchors in field tests at the site in Kentucky. According to Van Zaten, (1986), if the tension in a polyester geotextile is kept below 60% of its ultimate strength the problem of creep and stress relaxation in the geotextile is minimized. Therefore, to minimize creep and stress relaxation, the strength of the geotextile selected was such that when the loading from the ground anchor approached 60% of the strength of the geotextile the anchor

pullout capacity would be exceeded and the anchors would start to pullout. In addition, this allows for a continuous load on the soil in the case of slope movement, as noted by Vitton (1991).

It was decided that one 15 m (50 ft) by 24 m (80 ft) sheet of geotextile plus two cut sections of one 3.8 m (12.6 ft) by 30 m (100 ft) roll would be sufficient to stabilize the site. The polyester geotextile was sensitive to UV radiation, so to reduce the exposure of the geotextile to the sun, a thin sheet of a nonwoven Linq's Typar was placed over the entire installation and secured to the tops of the anchors and simply acted as a sacrificial material.

Anchors

Informal driving tests at the University of Alabama demonstrated that anchors could be driven sufficiently by a Hilte TE804 electric demolition hammer powered by a 4000 watt generator. The demolition hammer was used to strike a custom-made driver head threaded over the protruding end of the anchor as shown in Figure 5. As a contingency, extra driver heads were made to fit a 13 N (60 lb) pneumatic jackhammer that was rented, along with a compressor, if necessary.

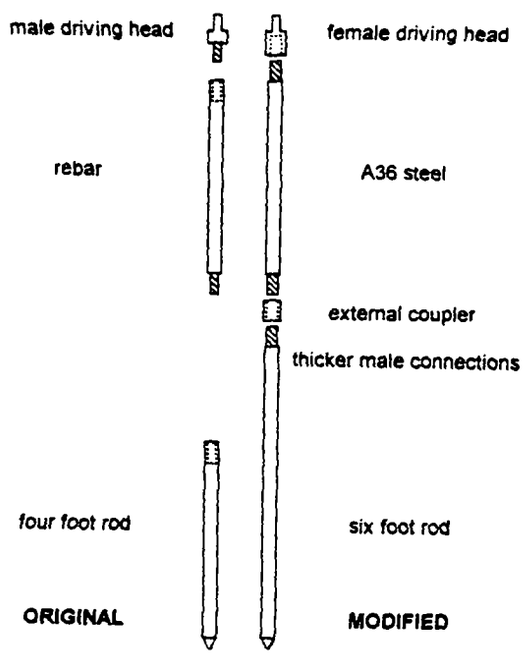

Figure 5. Anchor pattern used in the AGS.

Two anchor materials were considered: rebar and an A36 cold-rolled steel. Driving tests revealed that the rebar was too brittle for dynamic driving. The extreme vibrations caused by the impacts of the demolition hammer often caused the rods to twist apart or break. The cold-rolled steel rods, on the other hand, were more ductile due to the higher quality of steel. Therefore the rolled steel, despite being more expensive, was chosen over the rebar as the anchor material.

Since it is important to have the AGS anchors driven deep enough to penetrate the potential failure plane of a slope, a total anchor length of 3.9 m (13 ft) was chosen for the site based on an estimated maximum depth to the original failure plane of about two meters (7 ft). The total anchor assembly length consisted of four rods: (3) 1.2 m (4 ft) lengths and (1) .3 m (1 ft) length. The 0.3 m section was the last rod to be driven, and was threaded along its entire length to facilitate the assembly and tightening of the anchor-geotextile connection.

Early in the anchor testing process, the test rod lengths were manufactured with threaded male and female ends as illustrated in the left-hand portion of Figure 5. These rods could simply be twisted together without the need for any type of fastener or coupler. Driving tests showed that these unreinforced connections were vulnerable to shearing failure during driving. The new test rods were made with both ends turned down and threaded. These rods were connected by an external coupler as shown in the right-hand portion of Figure 5. This design proved sturdy, however, the jackhammer's dynamic driving action, which resulted in considerable vibrational movement of the top portion of the anchor, caused the anchor hole to enlarge at the surface. While this allowed room for the coupler, which had a somewhat larger diameter, to be driven into the soil, it also minimized the pullout resistance of the anchor since it prevented all but the first rod of the anchor assembly from having good contact with the soil. To minimize this problem, the first rod used in driving was increased from 1.2 m to 1.8 m (6 ft) in length as shown in Figure 5. The last section in the assembly was machined to a length of 0.6 m (2 ft) to maintain an

overall anchor length of 3.9 m.

Rod diameters of 13 mm (0.5 in.), 19 mm (0.75 in.), and 25 mm (1 in.) were tested at the University of Alabama to determine the relative pullout resistances of the three different sizes. These tests were conducted in a field on campus slated for construction, so good geotechnical information was available. The anchors were tested next to a Standard Penetration Test (SPT) hole that had N values ranging from 20 near the surface to 70 at resistance in a gravel layer at a depth of about 4.5 m (15 ft). The soil was a stiff clay with gravel lenses. Anchors of each size were driven to resistance with the Hilte TE804, then pulled out of the ground using a hydraulic lift or a forklift.

The 13 mm diameter rods tended to wander during driving, creating a hole that was not straight. This added to their pullout resistance, but the larger diameter rods had higher overall pullout resistance due to the increased soil-interface area. The demolition hammer was unable to effectively drive the 25 mm diameter anchor as deeply as the other anchors and were not considered further.

The 13 mm and 19 mm diameter rods were then field-tested at the research site in Kentucky using the Hilte TE804. Pullout results showed a significant increase in resistance for the 19 mm diameter anchors over the 13 mm rods and therefore 19 mm diameter rods were used in the installation.

For the remediation, the anchors would be driven 1.4 m (4.6 ft) apart in a hexagonal pattern as in Figure 6. Anchor driving was to begin in the center of the slide and proceed outward as shown in Figure 7.

Anchor-Geotextile Connections

The entire anchor geotextile connection assembly used in the installation is shown in Figure 8. The anchor geosynthetic connection cup was pressed out of one foot diameter, 14-gage steel circles to form bowls approximately 130 mm (5 in.) in maximum diameter and 50 mm (2 in.) deep. A 22 mm (0.875 in.) hole in the center of each of the connections allowed them to be placed on the .3 m, threaded section of the anchors. A flat 50 mm diameter area at the bases provided a contact surface for belleville springs. These springs were placed on the anchors between the anchor geotextile connections and tightening bolts in an attempt to maintain tension

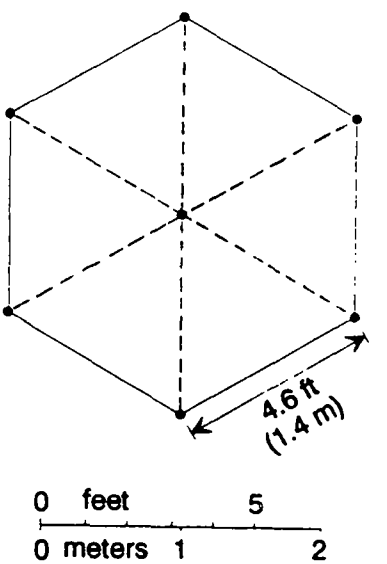

Figure 6. Hexagonal anchor arrangement.

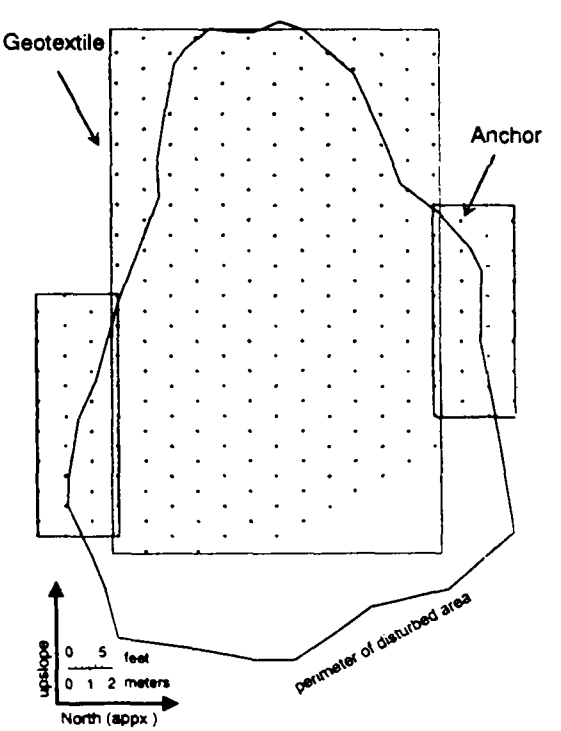

Figure 7. Anchor installation plan.

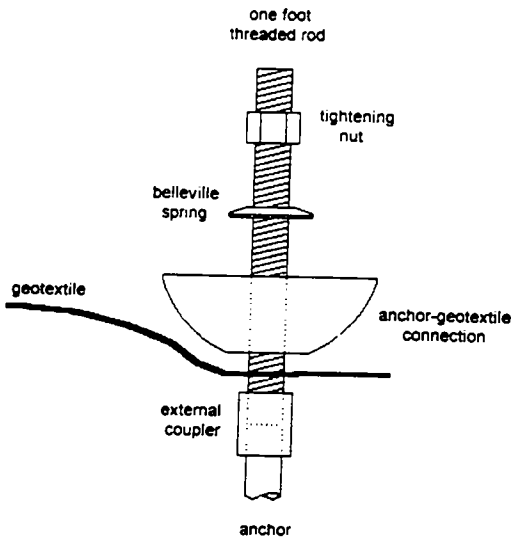

Figure 8. Anchor-geotextile connection.

on the geotextile in the event of geotextile creep or anchor movement. The tightening bolts were used to tension the AGS after anchor driving was completed and at later dates.

Installation

Installation of the AGS was started on December 1, 1993. A bulldozer was first used to placed the failed soil back up slope and to provide a more level surface for placement of the geotextile. Since some soil had been removed from the landslide in 1991, the bulldozer was unable to match the original volume and grade of the slope but did manage to adequately place the remaining material back up slope. It was very difficult in the upper portions of the slide due to very wet ground conditions, which at times were very soft. However, a relatively level surface was created in which to apply the AGS. Due to the smaller than expected area to be remediated, only the 15 m by 24 m geotextile was needed to secure the slope. Access to the landslide was limited, especially at the top of the slope, so it was necessary to manually place the fabric. Four people were able to lift the geotextile over a ditch, unroll it up the slope, and drag it into final position, though this was accomplished with difficulty.

As anchor driving began, all three available driver heads for the Hilte demolition hammer failed. At this time only seven anchors had been driven. A pneumatic jackhammer and associated driver heads were available, but considerable rain had begun to fall and the forecast for the next several days was poor. The installation was temporarily abandoned. Possible reasons for the unforeseen increase in driving resistance that caused the failure of the driving heads are the use of couplers, the unexpectedly shallow depth of soft fill over the stiffer, unfailed layer, and possibly the colder temperatures encountered in December as opposed to the temperatures in June when the field tests were conducted.

The first attempt to complete the AGS installation took place in March of 1994. This followed a very wet and snowy winter in which a portion of the slope beneath the geotextile, which had been placed in December, failed. Fortunately, however, it appeared that the seven anchors driven in December prevented this portion of the slope from completely failing downslope.

To complete the AGS installation a 13 N (60 lb) pneumatic jackhammer and diesel compressor was used in place of the electric demolition hammer and generator. The jackhammer was generally adequate for driving the ground anchors. The extensive sandstone fragments in the colluvium, however, caused difficulty in driving the anchors. Frequently, when the anchors encountered the sandstone fragments the anchor would either force the fragment out of the way or would penetrate through the fragment, which was indicated by difficult anchor driving followed by relatively easy anchor driving, i.e., the anchor would break through the fragment. In two cases, the anchors met resistance and could not be driven further. It was also observed that when an anchor hit a significant sandstone fragment, excessive vibrations would develop in the anchor causing additional enlargement to the anchor hole and reducing the anchor's pullout capacity.

The soil conditions below the geotextile ranged from firm at the base of the slide to extremely wet near the top of the slide. In some areas, even walking on the geotextile caused significant deformation of the geotextile. However, even in the very wet areas driving of the anchors resulted

in little to no general deformation of the soil between the anchors. Only very local deformation in the vicinity of the anchor occurred, which was generally within 30 cm or less of the anchor.

A total of four people completed the installation. One person worked ahead of the jackhammer laying out the anchor pattern using a fabricated triangular template which was 1.4 m (4.6 ft) on each side. By using this template the hexagonal anchor pattern could be properly positioned. This person would slide the anchor through the fabric making sure that the geotextile was not ruptured and then drive the first rod section as deeply as possible using a simple post-hole driver.

Two people were required to lift and operate the jackhammer due to the difficulties of working on a steep slope with a heavy jackhammer. A third person assisted by screwing on the driver head, guiding the jackhammer onto the head when it was lifted, and holding the driving head in place during driving since the head would often vibrate loose and damaging the rod threads if constant tightening wasn't maintained.

Because the depth of relatively soft, failed material was less than anticipated, anchor refusal during jackhammer driving occurred at depths less than the designed anchor length of 3.9 m. Most anchors in the completed system could only be driven 2.7 m (9 ft), while some anchors in the upper third of the AGS could only be driven 2.1 m (7 ft). The upper right corner of the AGS was unsecured because ground resistance in that area prevented the 1.8 m pointed rods from being driven completely, so the anchored geotextile connection could not be attached.

All but two of the anchors penetrated the shallow failure plane of the slope, though not by the 1.5 m (5 ft) suggested by Koerner (1990). Due to the difficulties in driving and the smaller area to be remediated, only 172 anchors were used to secure the slope as shown in Figure 9 then the planned 225 anchors.

Field Performance

Monitoring of the AGS included the use of anchor load cells, soil pressure gages, a rain gage, and a temperature probe. The purpose of these instruments was to record the responses of the AGS and the soil to the slope remediation process and changes in the weather. The site was also surveyed on a regular basis to detect any slope movement, and test anchors were driven at the base of the site to quantify any improvements in anchor pullout resistance over time. A Campbell Scientific CR10 datalogger was placed at the site in May of 1994 to monitor the instrumentation of the system. However, vandalism and power failures destroyed some of the data which was collected over several periods and totaled about three months throughout the monitoring period.

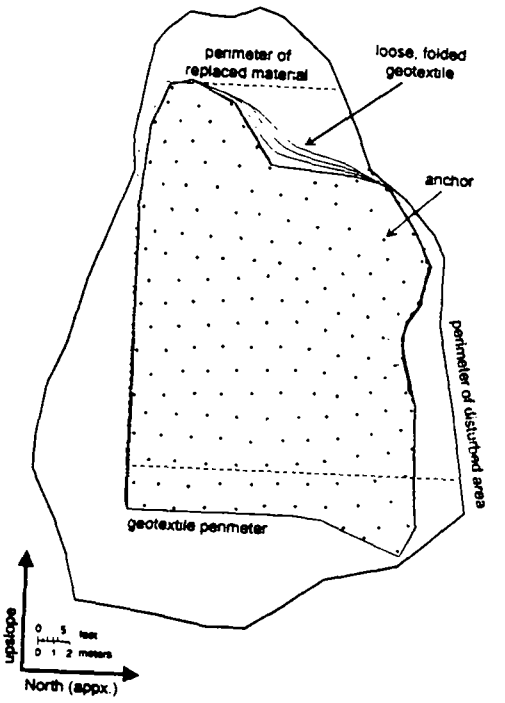

Figure 9. Completed AGS anchor layout.

A significant concern on anchor installation was that since the soils consisted of fine-grain materials, the initial pullout capacity of the anchor would be limited due to possible excess pore pressures build up during anchor driving, which would have to dissipate to achieve expected pullout capacity. Therefore, tensioning of the system was designed to be accomplished by the tightening bolt on each anchor sometime after the initial driving and not by the initial driving as suggested by Koerner (1984).

Nine load cells were installed to measure the tension in the anchors. This was done to determine the load that the anchors placed on the geosynthetic and whether or not this tensile load could be maintained over time. The load cells were fabricated from .3 m (1 ft) lengths of 19 mm diameter threaded steel as illustrated in Figure 10. After installation of the load cells, the assembly was tightened to tension the anchor and geosynthetic. The force in the anchor was recorded during and immediately after the tightening as well as for long-term changes.

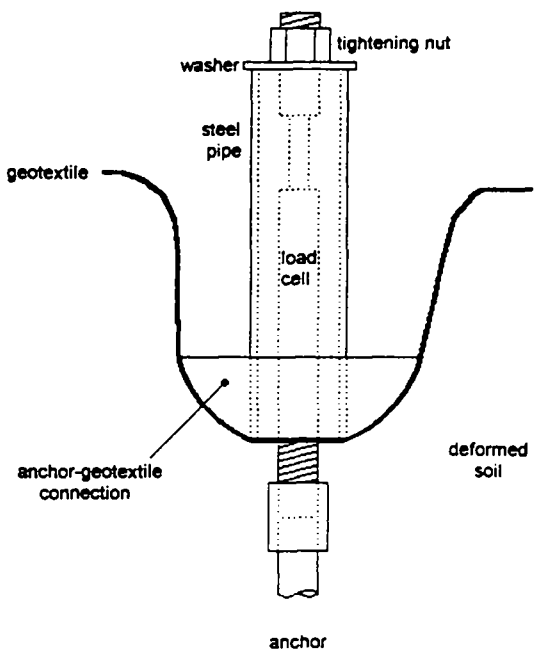

Figure 10. Anchor load cell design.

All load cells recorded an anchor load of between 110 N (500 lb) and 340 N (1500 lb) immediately after tightening. This load decayed to zero in ten to twenty days. An example of this is shown in Figure 11, where the loss in load occurs within 12 days. The load loss was believed to be due to geotextile relaxation or to local soil displacement, which resulted from soil consolidation in close proximity to the anchors, as opposed to pullout of the anchors, since anchor displacement measurements were made during tensioning that indicated little to no displacement of the anchor occurred at the time of loading. However, since the slope consisted of fine-grained soils it was also possible that soil creep along the length of the anchor could be responsible for the load loss.

After the AGS was completely installed, each anchor was tagged and numbered and surveyed using a laser theodolite. The site was first surveyed on July 11, 1994 and on an approximate two month intervals through July of 1995. The surveying showed negligible to no anchor movement for the entire monitoring period.

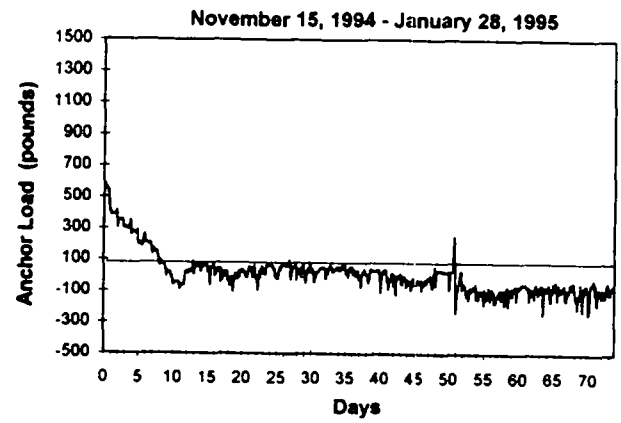

Figure 11. Anchor load versus time plot.

Anchor load changes in response to wet or dry periods were of interest as this could indicate potential slope movement in wet seasons or a shrink/swell phenomena, but no such changes were observed. However, increases of up to several hundred pounds were recorded during particularly cold weather. These spikes occurred in response to a sudden drop in air temperature to about -15° C. Closer inspection revealed trends of higher loads during colder weather and lesser loads during warmer spells. These changes are probably due to the thermal expansion and contraction of the imbedded steel anchors rather than any changes in the soil itself. The thermal changes in the steel also probably cause the daily fluctuations in load cell readings. In general, the loads reach a maximum overnight and quickly drop in the morning. This is consistent with the suspected thermal expansion and contraction of the anchors.

Before the placement of the geotextile, five soil pressure gages were installed approximately 0.6 m (2 ft) below the ground surface at various points along the slope. Three gages were

located beneath the geotextile and two gages were located below the geotextile perimeter and were not influenced by the AGS. All anchors were driven (the system was completely installed) before the datalogger was available to read the soil pressure gages. Therefore, it is not known if any pressure increases occurred during the tensioning of the geotextile over the slope. This is an important deficiency, as soil pressure increases would indicate possible soil consolidation, a major purported benefit of an AGS. However, two gages were relatively near load cell positions, where anchors were tightened on September and November of 1994. They recorded no apparent increase in soil pressure due to anchor tightening. This is consistent with the lack of deformation between the anchors, which is required to transfer the tension in the geotextile to a compressive load on the soil. While tension may exists in the geotextile, if no curvature develops through soil deformation then little to no compressive loading of the soil will result. For all of the anchors driven, only local deformation developed around the anchor with little to no deformation developing between the anchors. Therefore, there was insufficient curvature, r_c, or long term tension, N, in the geotextile to develop a compressive loading to the soil. While, all gages did show some increase in pressure due to rainfall events, the increases were small (typically less than 35 kPa (5 psi)), and were usually caused only with significant rainfall. It was concluded from the measurements made during this research, therefore, that the active stabilization of a slope by tensioning of the geotextile over the soil slope was not successful. However, based on the AGS's field performance, it is believed that other functions of the AGS did improve slope stabilization such as the effect of soil nailing from the anchors, halt of slope creep movement, and erosion control.

Conclusions and Comments

An abandoned mine land landslide located in Eastern Kentucky was remediated using an anchored geosynthetic system. Installation of the system took approximately two and half weeks utilizing four installation personnel although equipment failure and poor weather extended the installation to a period of four months. A high strength geotextile was used as the membrane and was anchored using steel ground anchors. The driving of the anchors was accomplished using a 13 N (60 lb) pneumatic jackhammer. The AGS was monitored using load cells, soil pressure cells, along with temperature and precipitation measurements over a period of about one year. Conclusions from this installation are as follows:

1. Although portions of the slope were very wet and soft, anchor driving was unable to deform the soil below the geotextile and thus minimal compressive loading was applied to the slope since limited curvature of the geotextile-soil interface developed.
2. Tensioning of the geotextile by the ground anchors was lost within ten to twenty days of application. The loss of load was believed to be a combination of soil consolidation immediately below the anchor-geotextile connection where most of the deformation occurred, and stress relaxation in the geotextile. Consequently, even if sufficient deformation developed, constant retensioning of the geotextile would be required.
3. While the AGS was not capable of functioning as an active remediation system, it did appear to function well as a passive remediation system, i.e., it prevented the slope from failing, which was in a relatively unstable state especially during wet periods, although the monitoring period was not sufficient to confirm that the system would function well into the future.
4. Driving of the anchors in the colluvial soil was difficult at times due to the presence of sandstone fragments. It was also observed that in the driving process the anchor hole would be enlarged due to the vibrations induced in the anchor. Therefore, the top portion of the anchor was not in contact with the soil. This effect was further enhanced when sandstone fragments were encountered at depth and the anchor vibrations significantly increased as the anchor attempted to break through the rock

fragment. An additional consideration on anchor driving is the build up of excess pore pressure, which reduces the pullout capacity of the anchor and makes tensioning the system difficult during anchor driving.

5. The affect of the ground anchors acting as soil nails appears to be effective but was not quantified in this research. Also, the geotextile as expected provided erosion control for the slide area.

While the results of this research are mixed, it is believed that AGS may provide an effective remediation system for certain types of slopes prone to creep. Further research, however, is needed to determine the ability of AGS to halt progressive slope failure for slopes consisting of heavily overconsolidated soils that exhibit strain-softening behavior leading to creep failure. Since colluvial soils commonly consists of these types of soil, it is believed that anchored geosynthetic systems may provide a possible remediation system for these types of slopes.

Acknowledgment

This research was sponsored by the United States Bureau of Mines under the Abandoned Mine Lands Program and administered through Contract No. 1432-J0230005 titled "The Application of Anchored Geosynthetic Systems for Abandoned Mined Land Landslide Remediation." In particular, the authors would like to thank Mr. Tony Iannacchione, the technical project officer for his support, encouragement, and timely advise throughout the project. The financial and moral support are gratefully acknowledged.

Literature Cited

Greenwood, J. R. 1985. Geogrids and Anchors for Slope Stabilization - Simple Method of Analysis. Proceedings of the 11th International Conference on Soil Mechanics and Foundation Engineering, Discussion, Vol. 5, pp. 2770-2771.

Koerner, R. M. 1984. Slope Stabilization Using Anchored Geotextiles: Anchored Spider Netting. Proceedings, Spec. Engineering for Roads and Bridges Conference, PennDot, Harrisburgh, PA.

Koerner, R. M. 1985. Load Transfer Considerations Using Geotextiles. Geotechnical Fabrics Report, IFAI, Vol. 3, No. 2, pp. 11-14.

Koerner, R. M. 1986a. Designing with Geosynthetics. Prentice-Hall, Englewood-Cliffs, NJ, pp 118-123.

Koerner, R. M. 1986b. A New Method of Soil Slope Stabilization Using Geosynthetics. Geotechnical Fabrics Report, IFAI, Vol. 4, No. 1, pp. 18-25.

Koerner, R. M. and Robbins, J.C. 1986c. In-situ Stabilization of Slopes Using Nailed Geosynthetics. Proceedings, Third International Conference on Geotextiles, Vienna, Austria, April 7-11, pp. 395-400.

Iannacchione, A. T., Bhatt, S. K., and J. Sefton 1994. Geotechnical Properties of Kentucky's AML Landslide and Slope Failure Evaluation. Proceedings, 16th Annual Conference of the Association of Abandoned Mine Land Programs, Park City, Utah, September 18-21, 1994.

Van Zaten, R. V. 1986. Geotextiles and Geomembranes in Civil Engineering. Wiley & Sons, New York, USA.

Vitton, S. J. (1991), "An Experimental Investigation into the Load Transfer Mechanism in Anchored Geosynthteic Systems, Thesis presented to The University of Michigan, at Ann Arbor, MI, in partial fulfillment of the requirement for the degree of Doctor of Philosophy.

MAXIMUM SAFE SLOPE ANGLES FOR PROPOSED SHIPLOCKS OF THE THREE GORGES DAM SITE BASED ON KINEMATIC ANALYSES PERFORMED ON MAJOR DISCONTINUITIES

by

Jeong-gi Um[2], Pinnaduwa H. S. W. Kulatilake[3], Jianping Chen[4], and Jianren Teng[5]

Abstract. The Three Gorges Project has been proposed to harness the great hydrologic power potential of the Yangtze River, which is the largest river in China. The depth of rock excavation needed to construct the permanent navigation structures (shiplocks) is high, with a maximum of 170m in some locations. The granitic rock mass which exists in the shiplock region contains a number of major discontinuities and about four sets of minor discontinuities. One hundred and thirty three major discontinuities have been mapped around the shiplock covering an area of 1740×600m. Kinematic analyses were conducted using the major discontinuities to estimate maximum safe cut slope angles with respect to plane sliding, wedge sliding and toppling failure. Kinematic analysis for plane sliding has resulted in maximum safe cut slope angles greater than 65° for most of the discontinuities. For most of the wedges, maximum safe cut slope angles greater than 45° were obtained. Maximum safe slope angles greater than 85° were obtained for most of the discontinuities in the toppling case. It seems that the shiplock faces in the proposed permanent shiplock region in fresh rock are stable up to a cut slope of about 45°. However, it is important to keep in mind that this conclusion is based on the kinematic analyses performed using only the major discontinuities. Further kinematic as well as kinetic analyses are recommended incorporating minor discontinuities, water forces, earthquake forces, etc., before making the final conclusions about maximum safe cut slope angles for the shiplock region.

Additional Key Words: Rock, Slope Stability.

Introduction

The Yangtze River is the largest river in China. From its headwaters to its estuary, the Yangtze River meanders over 6,300 km (Fig. 1) and its annual runoff into the sea amounts nearly 1,000 billion m^3 (Ha 1993). Its total drop is more than 5,800 m with a water power potential of up to 268,000 Mw. In order to harness the river and develop its water resources, extensive efforts in investigation, planning, design and scientific research have been conducted for nearly forty years. The Three Gorges Project has been proposed in order to exploit the great hydroelectric power potential of the Yangtze River. The project has tremendous multi-purpose benefits such as flood control, electric power generation, navigation, irrigation, tourism and fishery enhancement.

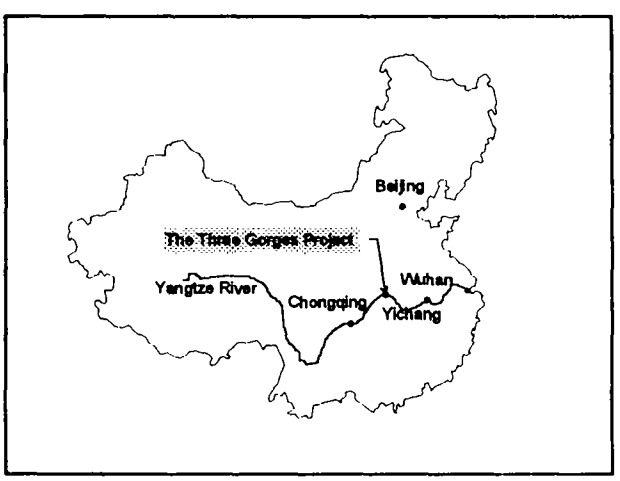

Figure 1. Geographical positions of Yangtze River and Three Gorges project in China.

1. Paper presented at the 1996 National meeting of the American Society for Surface Mining and Reclamation, Knoxville, Tennessee, May 18-23, 1996.
2. Graduate Student, Department of Mining and Geological Engineering, University of Arizona, Tucson, AZ 85721
3. Associate Professor, Department of Mining and Geological Engineering, University of Arizona, Tucson, AZ 85721
4. Visiting Scholar from Changchun University of Earth Sciences, China.
5. Visiting Scholar from Yangtze Water Resources Commission, China.

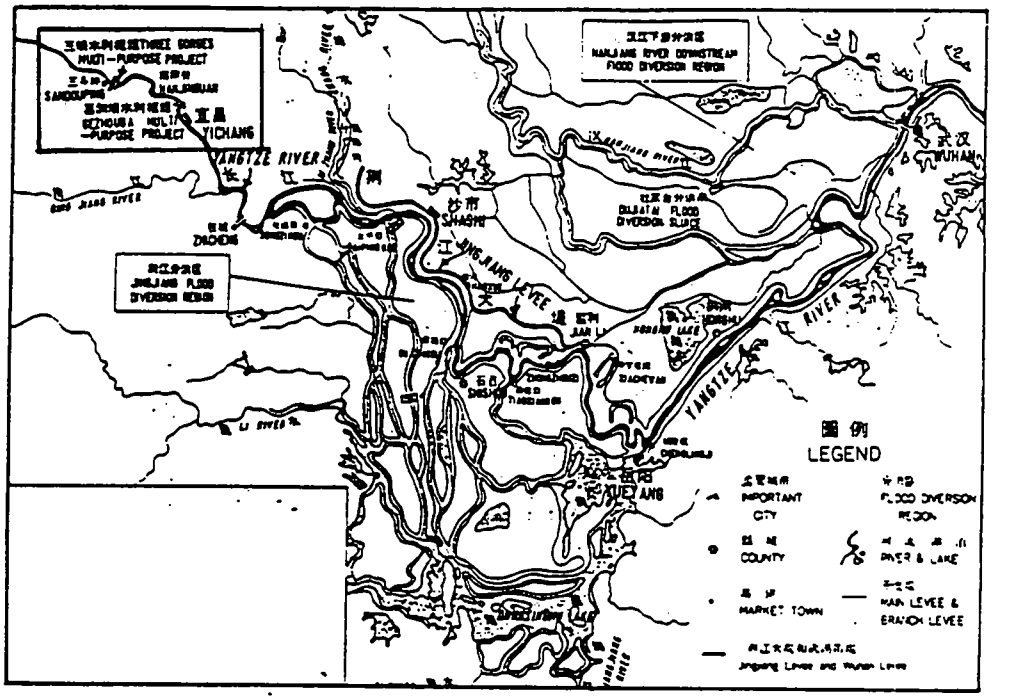

Figure 2. Locations of the planed Three Gorges Project and the completed Gezhouba project on the Yangtze River, China.

The river stretches from Fengjie to Yichang, about 200 km, and cuts through three majestic canyons, Qutang Gorge, Wuxia Gorge and Xiling Gorge - known as the Three Gorges. The Three Gorges Project is located in the middle of Xiling Gorge, about 40 km upstream of the Gezhouba water conservancy project which was completed in 1988, with its dam site at Sandouping in Yichang, Hubei Province (Fig. 2). The construction of Gezhouba dam was done not only with the aim of gaining the immediate benefits from electricity generation and navigation improvement, but also as a rehearsal for the construction of the proposed Three Gorges Project. The China Three Gorges Project Development Corporation, established in 1984, is in charge of the construction of the gigantic project. The Yangtze (Changjiang) Water Resource Commission (formally Yangtze Valley Planning Office) is in charge of the investigation, planning and design of the project (Chen 1986).

The project is composed of concrete dams, flood discharging facilities, power houses, sluice outlets, and navigation structures (Fig. 3). The concrete gravity dam will have a crest length of 2000m and a maximum height of 175m. The expected total reservoir storage capacity is 30.93 billion m^3. The normal water depth of the three Gorges reservoir is expected to be around 175m. The total generating capacity of the power stations will be about 18,200 Mw. The permanent navigation facilities will be located on the left bank, consisting of a five-stage double-lane shiplock (Fig. 4) with effective dimensions of 280 x 34 x 5 m (length x width x water depth) and a one-way shiplift with effective dimensions of 120 x 18 x 3.5 m. During the construction period, a temporary one-way shiplock is scheduled to be built (Fig. 3). The project construction began in October 1993. The total estimated construction time for the project is 18 years. For further details related to the project construction, the reader is referred to the report by Ha (1993). The dip direction (with respect to North) of the downstream axis of the permanent shiplock is 111 degrees. The depth of rock excavation needed to construct the permanent shiplocks is high with a maximum of 170 m in some locations. Operational

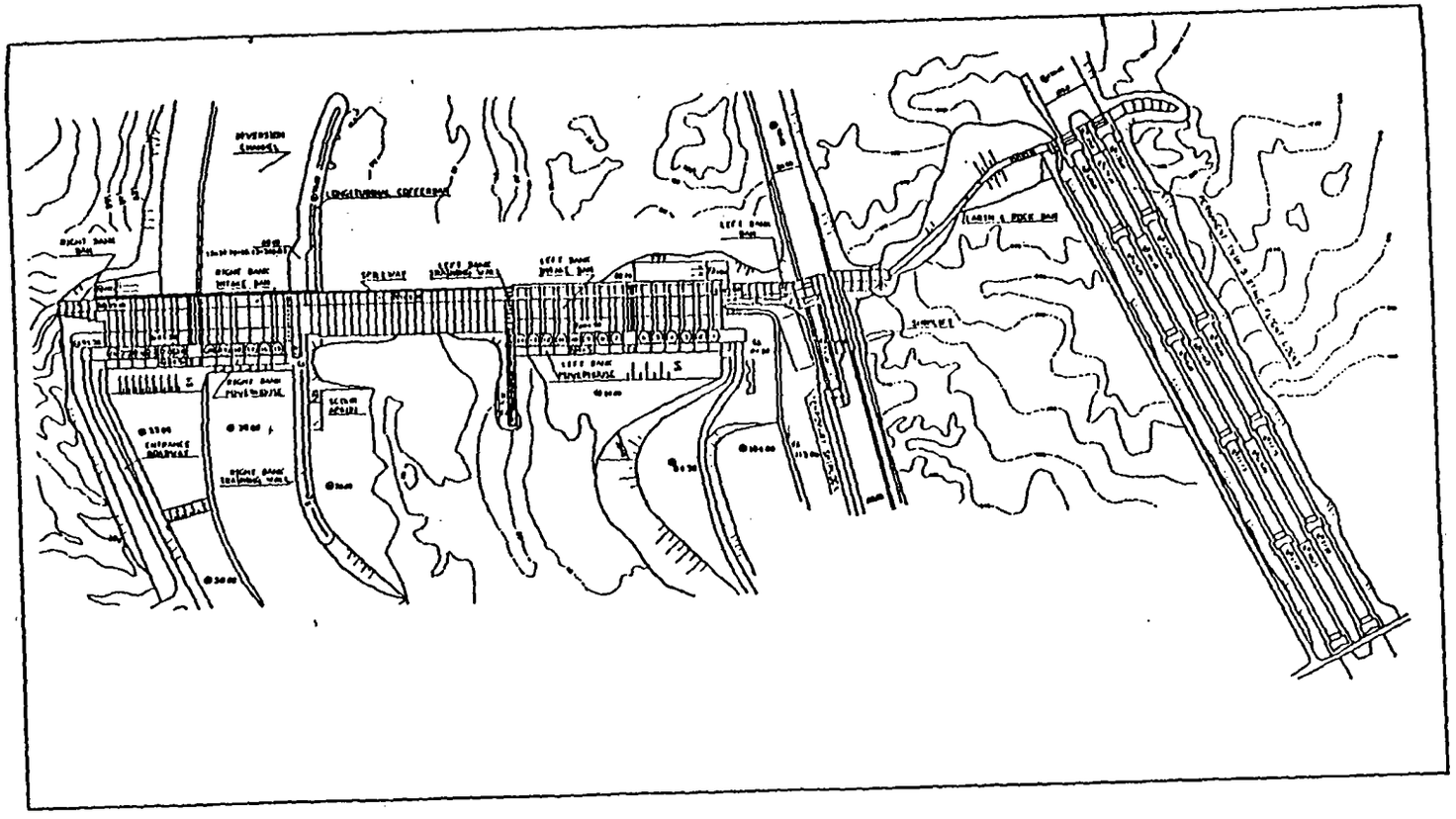

Figure 3. Layout of the Three Gorges Project [after Ha(1993)].

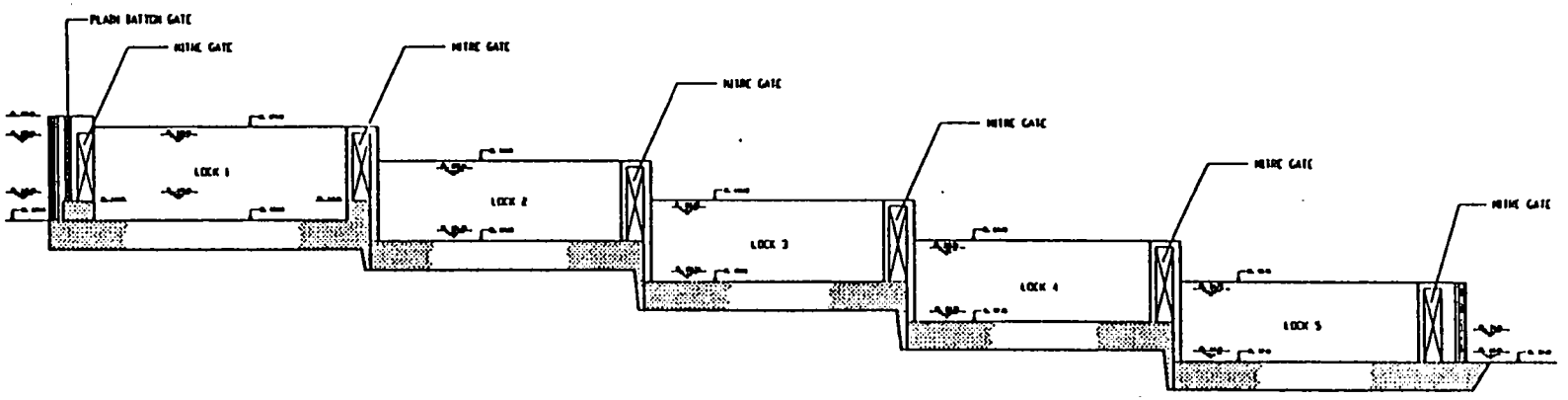

Figure 4. A vertical sectional view of the permanent shiplocks [after Ha(1993)].

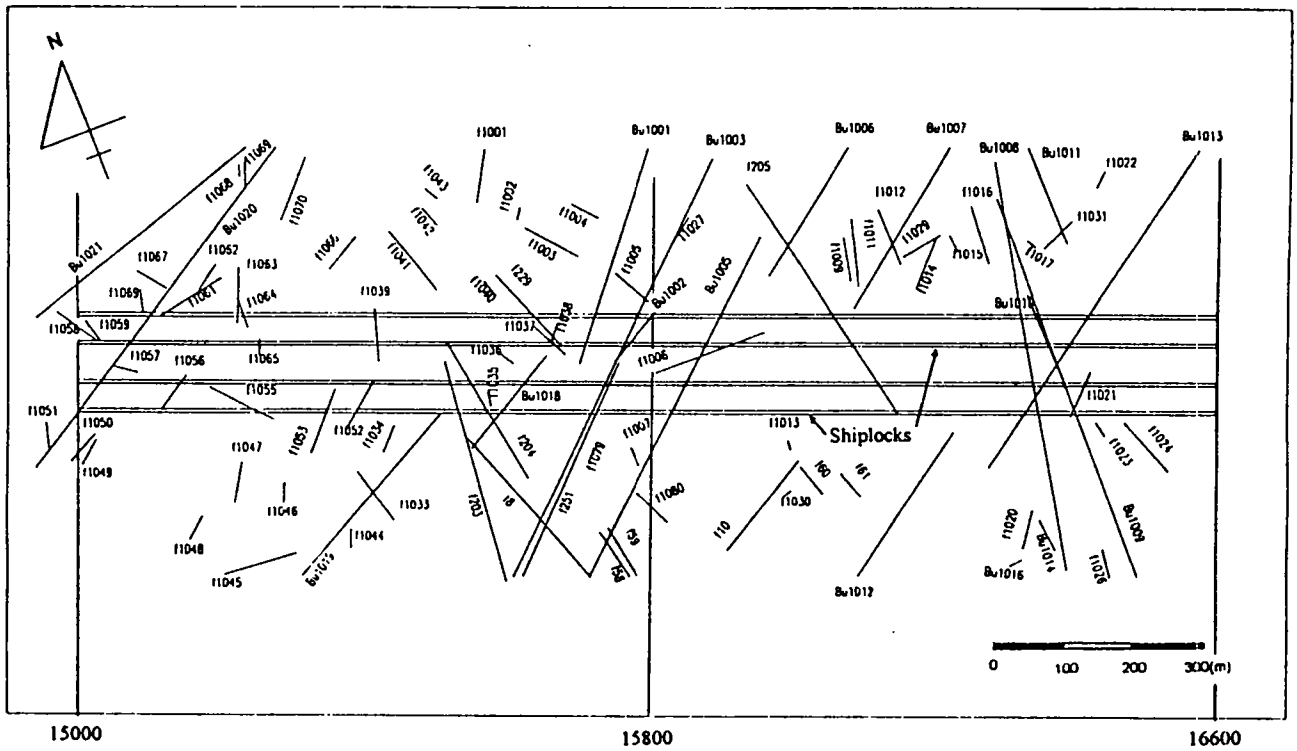

Figure 5. Major discontinuities in the proposed permanent shiplock area.

conditions of the shiplocks demand steep rock slopes on either side of the shiplocks which are about 1600 m long (Fig. 5). The granitic rock mass which exists in the shiplock region contains a number of major discontinuities, and a number of sets of minor discontinuities. Therefore, The rock engineering problems of high, steep rock slopes in the shiplock region are very complicated. Rock mass failures in the shiplock region must be fully prevented to assure safe travel of people in the ships and flood-free conditions downstream. Therefore, it is important to devise a design scheme to provide stable, steep, high rock slopes in the shiplock region. To achieve this ultimate goal, the first step was to characterize the discontinuity network in the rock mass close to the proposed permanent shiplock region (Kulatilake et al. 1996). This was done using about 2050 discontinuity trace data as mapped on the walls and the roof of a 400 m tunnel which is located close to the proposed shiplock region. This paper describes the second step performed towards reaching the ultimate goal. Note that further research is necessary to reach the ultimate goal.

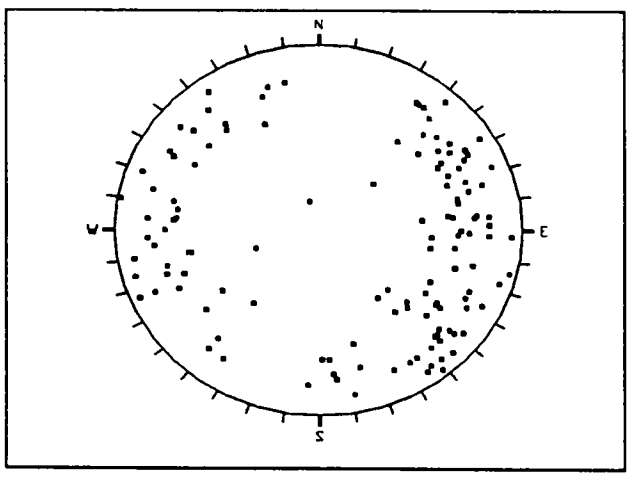

Figure 6. Orientation distribution of major discontinuity poles in the shiplock area on a lower hemisphere equal-area polar diagram.

Geology

Comprehensive geological research for the Three Gorges Region has been in progress since 1950s and is still continuing. The dam site of the Three Gorges Project is situated in the south part of the Huanglin anticline. The Huanglin anticline is 72 km long along the north-south (NS) direction and 35 km wide. It consists of crystalline rock masses of a presinian system. The major rock type is Huanglin granite (hornblend-biotite-plagioclase granite) which

is about 90% of the total area of the dam site, with the other being diorite. There are many intrusive dikes in the rock mass. The fresh granite and diorite are hard, with saturated compressive strengths around 100 MPa and 140 MPa, respectively. The ground surface has been seriously weathered. The thicknesses of weathered layers are different in ridges and ravines with an average thickness of 20-40 m. According to the degree of weathering, the rock mass is classified into 4 types (Wang 1986): (a) completely weathered, (b) strongly weathered, (c) weakly weathered, and (d) slightly weathered and fresh rock. The major rock type in the shiplock area is granite with the other being diorite. Diabase, quartzose and pegmatite can be found in the dikes or reefs. Also, lenses of Horneblende Schist can be found.

Major Discontinuities (Faults and Dikes) in the Proposed Shiplock Region

One hundred and thirty three major discontinuities have been mapped around the permanent shiplock covering an area of 1740x600m. Figure 5 shows the locations as well as the strike directions for these major discontinuities. Figure 6 shows the pole distribution of these major discontinuities on a lower hemispherical equal-area polar diagram. High orientation variability of the major discontinuities is well depicted by the polar diagram. Predominant strike directions of the major discontinuities seem to be along NEE-SWW and NW-SE directions. Most of them have steep dip angles varying between 60-70°. The lengths of most of these major discontinuities are expected to be between 50 and 100m. The friction angle (ϕ_j) values of the major discontinuities range from 35° to 45°. To obtain conservative results, the minimum value of ϕ_j of 35° was used in the performed kinematic analyses.

Kinematic Analyses

"Kinematic" refers to the motion of bodies without reference to the forces that cause them to move (Goodman 1989). Kinematic analyses are very useful to investigate possible failure of rock masses which contain discontinuities. Failure involving movement of rock blocks on discontinuities combine one or more of the three basic modes-plane sliding, wedge sliding and toppling. For the proposed permanent shiplock region, kinematic analyses were performed to estimate maximum safe slope angles with respect to the aforementioned three basic failure modes. The basic concepts related to estimation of maximum safe slope angles for the three basic modes of failure are briefly explained below.

Plane Sliding

Consider the case of plane sliding under gravity alone as shown in Fig. 7(a). Any block tending to slide on a single plane surface will translate down the slope parallel to the dip of the discontinuity. If a cut slope is inclined at an angle α to the horizontal, the conditions for a plane slide are that the dip vector of the discontinuity, D, be pointed into the free space of the excavation and plunge at an angle less than α. If δ is greater than α, the block will be stable and no sliding will take place.

This concept can be represented on the stereographic projection (Fig. 7(b)). The cut slope can be constructed as a great circle in the lower hemisphere. D_1 is the dip vector of discontinuity plane 1, and D_2 is the dip vector of discontinuity plane 2. δ_1 and δ_2 are dip angles of planes 1 and 2, respectively. In this example, δ_1 is less than α, and therefore, plane 1 would allow a plane slide. On the other hand, δ_2 is greater than α and plane 2 would not allow a plane slide. In other words, if the dip vector of the discontinuity plane lies in the shaded region, then the plane would allow a slide. The limiting situation arises when the great circle of the cut slope passes through the dip vector of the discontinuity plane. When this occurs, the dip angle of the cut slope corresponds to the maximum safe slope angle with respect to plane sliding.

Figure 7(c) shows the reverse situation. If the dip vector of a discontinuity surface is known, it is possible to determine the maximum safe slope angle corresponding to a cut of assigned strike. The maximum safe slope angle α is the dip of the great circle passing through the given strike and the known dip vector D.

It is important to note that in the case of plane sliding under self weight alone, failure can occur only if the surface of sliding dips steeper than ϕ_j. Therefore, in a lower hemispherical stereographic projection, if a dip vector D of a discontinuity lies in the shaded area in Fig. 7(d), plane sliding will not occur under any cut slope angle. That means the corresponding maximum safe cut slope angle is 90°. Thus, it is necessary to use the concepts shown in both Figs. 7(c) and (d) in estimating the maximum safe cut slope angles under the plane sliding situation.

Wedge Sliding

Sliding along a line of intersection occurs when two discontinuity planes intersect to make a wedge. Figure 8 shows how to obtain graphically the

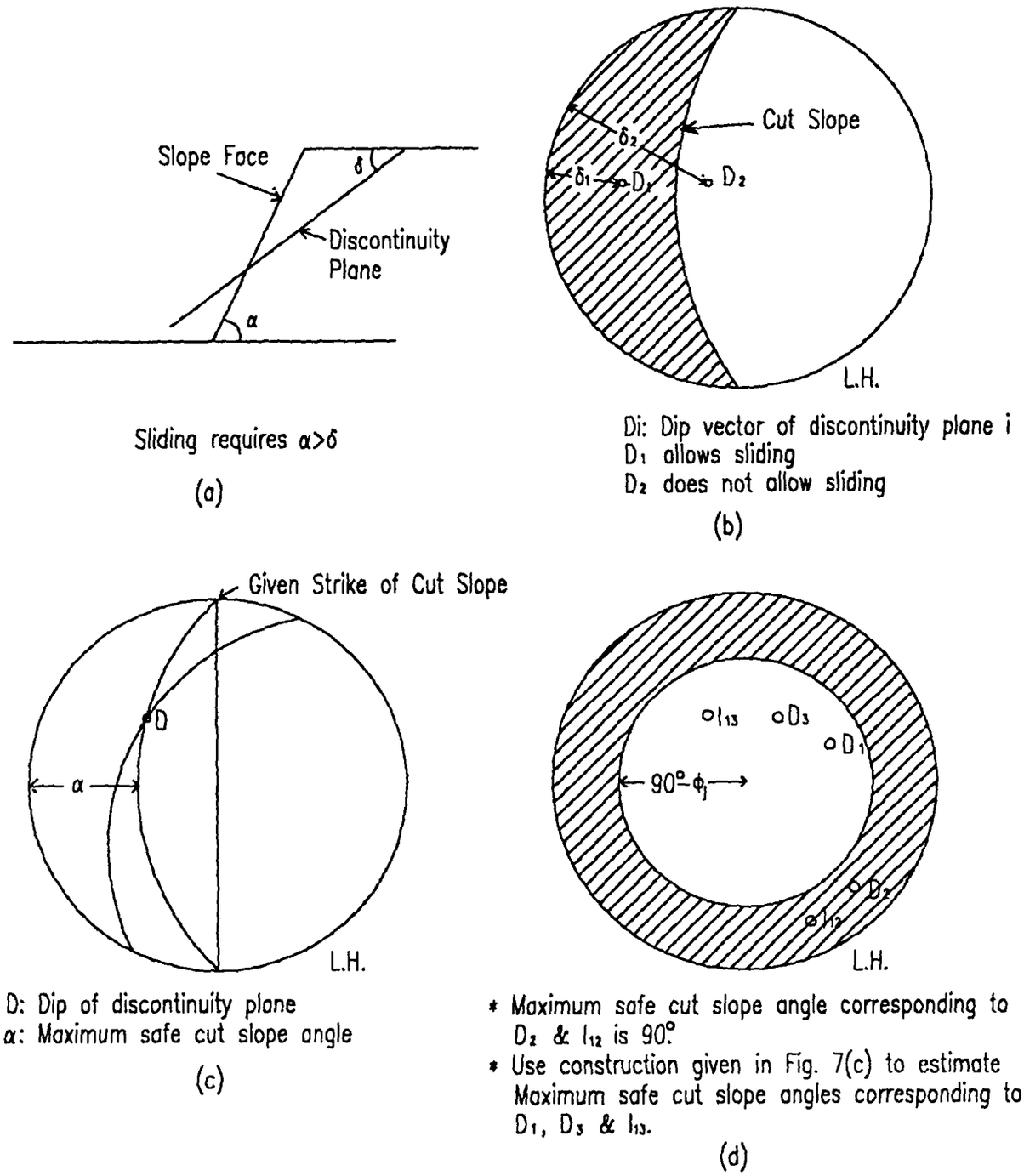

Figure 7. Concepts related to kinematic analysis for plane sliding [Goodman(1989)] (a) daylighting requirements on a pictorial diagram. (b) daylighting requirements on a stereographic plot. (c) great circle for cut slope providing the maximum safe slope angle. (d) influence of ϕ_j on maximum safe cut slope angle.

maximum safe cut slope angle for a possible sliding wedge. When discontinuity planes 1 (P1) and 2 (P2) make a wedge, the maximum safe slope angle for a cut slope of assigned strike can be found in a similar way to the plane sliding case. If the cut is made with the strike as shown in the figure, the maximum safe slope angle α is obtained by the dip of the great circle which passes through the intersection of planes 1 and 2 (I_{12}) and the points corresponding to the assigned strike.

Note that Fig. 7(d) is equally applicable for wedge sliding situation. If the line of intersection of two discontinuity planes, I_{ij}, lie in the shaded area in Fig. 7(d), then the maximum safe cut slope angle corresponding to I_{ij} is 90°. Thus, the concepts shown in Figs. 7(d) and 8 should be used in estimating maximum safe cut slope angles under wedge sliding situation.

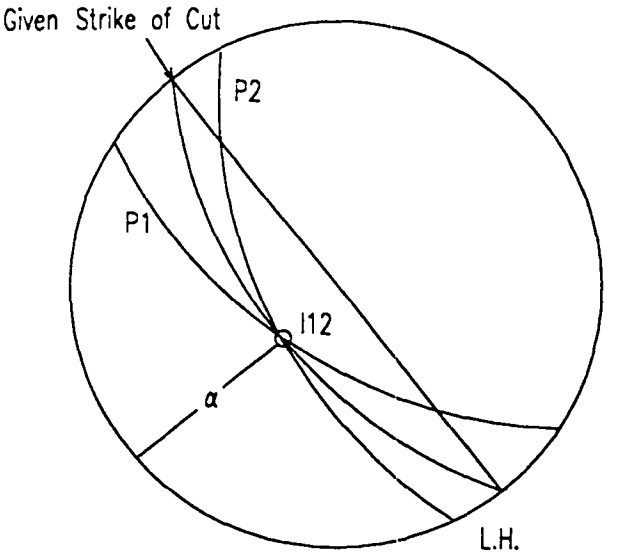

α: Maximum safe cut slope angle

Figure 8. Stereographic construction to obtain the maximum safe slope angle for wedge sliding.

Toppling

Fig. 9 illustrates the kinematic analysis for toppling under gravity alone. Toppling can occur only if the discontinuities strike nearly parallel to the strike of the slope, say within 30°. In addition, discontinuity spacing should be low as shown in Fig. 9(a) to form thin layers of rock. For toppling failure, first it is necessary to initiate interlayer slip before large flexural deformations take place within the layers. If the layers have angle of friction ϕ_j, slip will occur only if the direction of applied compression (which is along the dip vector of slope) makes an angle greater than ϕ_j with the normal to the layers. If the cut slope is inclined α to the horizontal and the dip of discontinuity planes is δ, then the kinematic requirement for toppling is $(90-\delta) + \phi_j < \alpha$ as shown in Fig. 9(a). On a lower hemispherical stereographic projection, for toppling failure to occur, the normal vector N of the discontinuity should lie within the shaded area as shown in Fig. 9(b). The situation corresponding to the maximum safe cut slope angle occurs when N falls on the great circle which is ϕ_j degrees below the cut slope and striking parallel to it. Note that when N lies outside the two small circles shown in Fig. 9(b), the corresponding maximum safe cut slope angle is 90°. Also, it is important to note that toppling can occur only on discontinuities whose normals plunge at an angle less than $90-\phi_j$. That means with respect to the lower hemispherical stereographic plot shown in Fig. 9(c), if a normal vector of a discontinuity lies within the shaded area shown in Fig. 9(c), then the corresponding maximum safe cut slope angle is 90°. Thus, the concepts shown in both Figs. 9(b) and 9(c) should be used in estimating the maximum safe cut slope angles for toppling mode. Also, it is important to check whether the discontinuity geometry produces thin rock layers as shown in Fig. 9(a).

Results

Kinematic analyses were conducted using the mapped major discontinuities in the shiplock area to estimate maximum safe slope angles with respect to possible plane sliding, wedge sliding and toppling failure. Each major discontinuity was treated as a single feature. A computer code KINEM was developed to calculate maximum safe slope angles. Eventhough the mapped major discontinuities are shown in Fig. 5, some uncertainty exist concerning the actual extent of these discontinuities. Therefore, the kinematic analyses were conducted under two different cases as given below. For case 1, orientation of all the major discontinuities which appear on Fig. 5 were considered in the kinematic analyses. Under this case, indirectly, it was assumed that any major discontinuity appearing on Fig 5 has a possibility to cross the shiplock. Thus, results from these analyses can be considered to be on the conservative side. The major discontinuities which only crosses the shiplocks according to Fig. 5 were used in the kinematic analyses in the second case. If the major discontinuity map given in Fig. 5 is reliable, then these analyses should provide results closer to the reality.

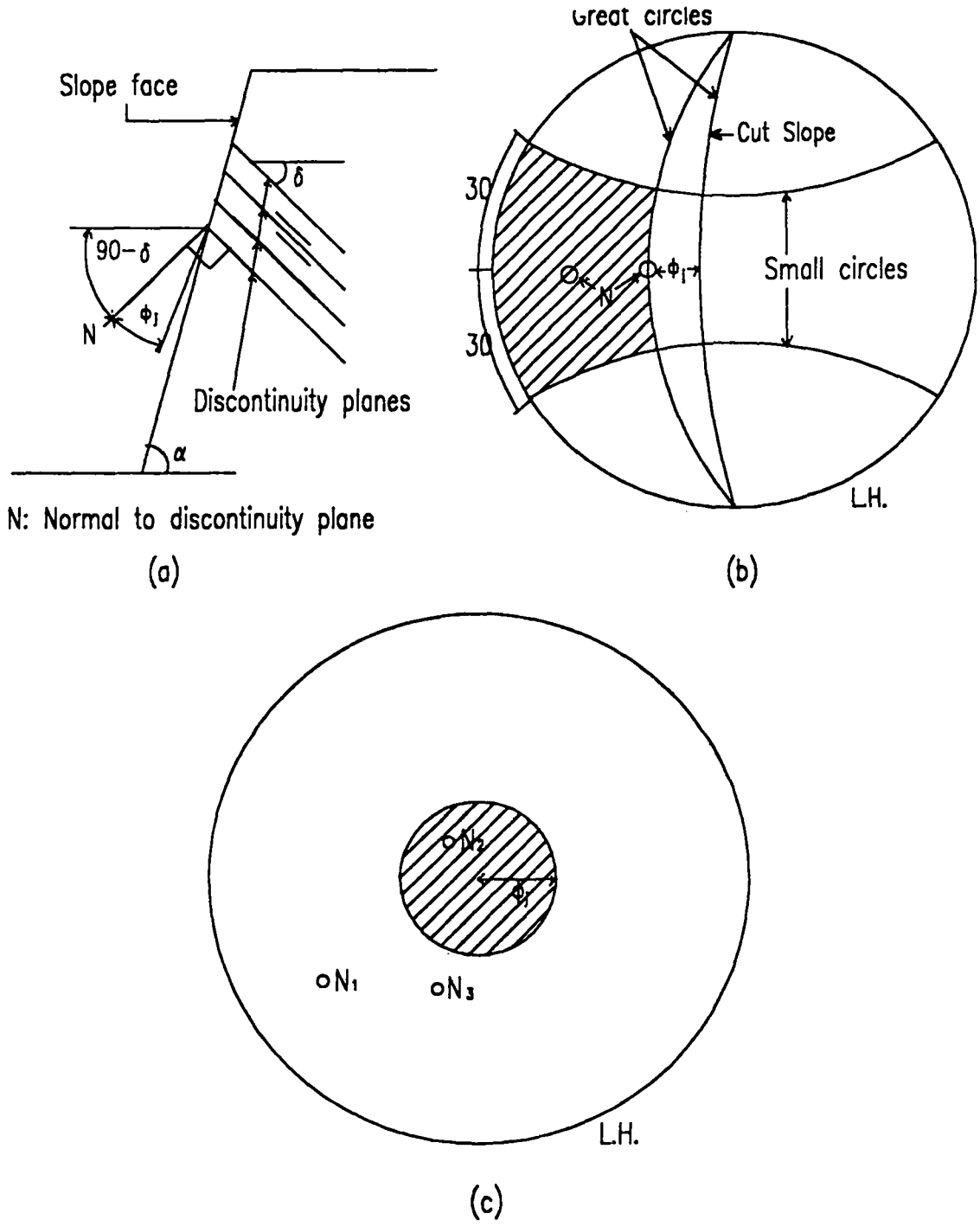

* Maximum safe cut slope angle corresponding to N_2 is 90°
* Use construction given in Fig. 9(b) to estimate maximum safe cut slope angles corresponding to N_1 & N_3

Figure 9. Concepts related to kinematic analysis for toppling [Goodman(1989)] (a) a pictorial diagram. (b) on a stereographic plot. (c) influence of ϕ_j on maximum safe cut slope angle.

For Case 1 :

Plane Sliding. The maximum safe slope angle obtained for each major discontinuity is shown in Figs. 10(a) and (b), respectively for cut strike directions 111° (South-West shiplock face) and 291° (North-East shiplock face). The location of each bar shown in Fig. 10 corresponds to the actual location of the major discontinuity in the shiplock area. The starting and ending points of each bar represent starting and ending X coordinates of each major discontinuity. Note that X axis coincides with the strike of shiplock faces. Therefore, the location of each major discontinuity and the maximum safe slope angle corresponding to it can be identified from this diagram. Most of the bars in Figs. 10(a) and (b) indicate maximum safe slope angles between 65° and 90°. The results obtained for the whole shiplock region (disregarding the actual locations of major discontinuities) are shown through histograms in Fig. 11(a). Most of the maximum safe slope angles were found to be greater than 65°.

Wedge Sliding. For the wedge sliding mode, only the discontinuities which are located within a 50m distance were considered in calculating the maximum safe slope angles. Results for individual wedges are shown in Figs. 10(c) and (d). Similar to Figs. 10(a) and (b), each bar represents starting and ending X coordinates of each wedge. Figure 11(b) shows the histograms obtained for the maximum safe slope angle for the whole shiplock region disregarding the actual locations of the wedges in the shiplock area. For most of the wedges, maximum safe cut slope angles greater than 45° were obtained.

Toppling. It is not really necessary to consider toppling mode for the shiplock region since it is covered by a granitic rock mass. Toppling failures usually occur in layered rock such as slate, schist, and sedimentary rocks, and chances to form thin layers in a granitic rock mass are extremely low. Anyway, in this study, kinematic analysis was conducted for toppling. Due to the aforementioned reasons, these results should be considered as highly conservative estimates. Results for individual discontinuities are shown in Figs. 10(e) and (f). Figure 11(c) shows the histograms obtained for the maximum safe slope angle for the whole shiplock region disregarding the actual locations of the major discontinuities in the shiplock area. Most of the maximum safe slope angles for the toppling case were found to be greater than 85°.

Table 1 Major discontinuity orientation data for different segments of the shiplock for case 2 kinematic analyses.

15150-15200(m)	Strike of SW Shiplock Face: 111°	
Discontinuity	Dip	Dip Direction
1. βu1020	82	316
2. F1062	60	326
3. F1061	75	351
4. F1067	80	46
15550-15600(m)	Strike of NE Shiplock Face: 291°	
Discontinuity	Dip	Dip Direction
1. F203	70	262
2. F204	82	45
3. βu1018	80	331
4. F1035	84	285
5. F8	80	247
15750-15800(m)	Strike of SW Shiplock Face: 111°	
Discontinuity	Dip	Dip Direction
1. βu1001	78	300
2. F1005	80	221
3. βu1002	80	325
4. βu1003	50	320
16080-16130(m)	Strike of SW Shiplock Face: 111°	
Discontinuity	Dip	Dip Direction
1. F205	65	269
2. F1009	80	274
3. F1011	70	101
4. βu1007	85	329
16420-16470(m)	Strike of NE Shiplock Face: 291°	
Discontinuity	Dip	Dip Direction
1. F1021	80	306
2. F1023	76	78
3. F1024	70	251
4. βu1009	78	90

F: fault, βu: dyke
Orientations of Cut Slopes:
Strike of Cut (SW shiplock face) = 111°
Strike of Cut (NE shiplock face) = 291°
Dip Direction of SW shiplock face = 201°
Dip Direction of NE shiplock face = 21°

For Case 2 :

The total length of the shiplock (1750m) was divided into 50m segments. Those segments which do

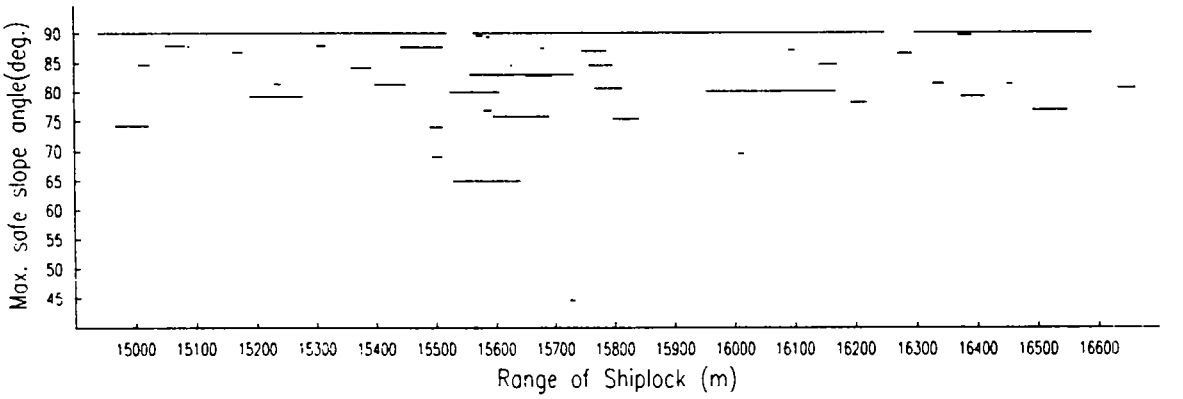

(a) Plane Sliding - Cut Dir.=111°

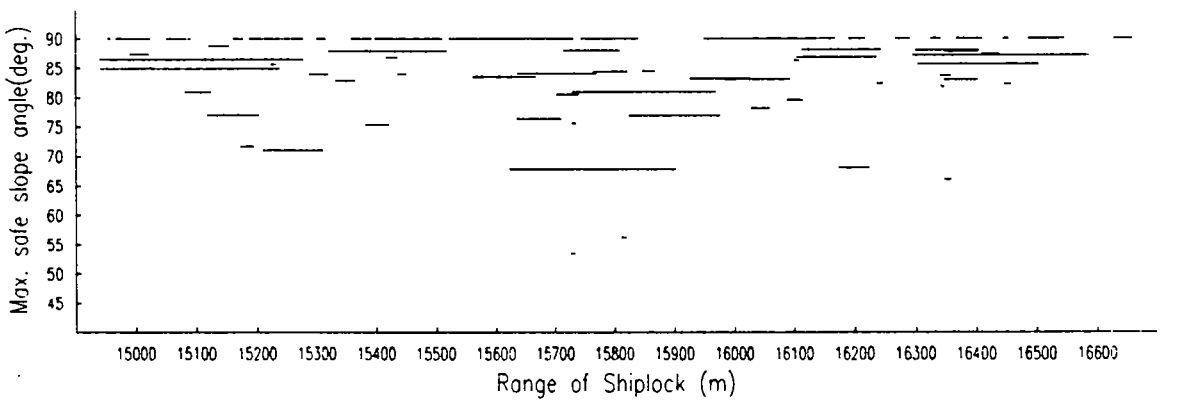

(b) Plane Sliding - Cut Dir.=291°

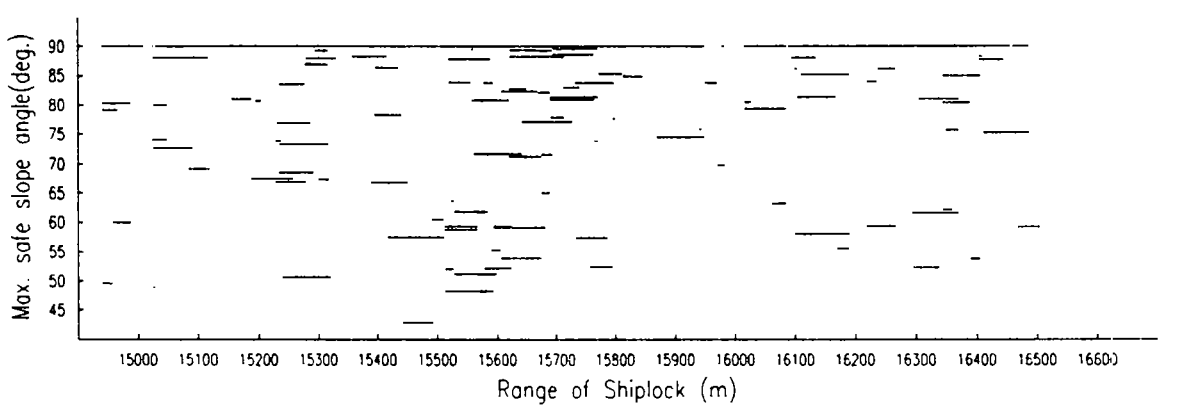

(c) Wedge Sliding - Cut Dir.=111°

Figure 10. Maximum safe slope angles along shiplocks resulting from kinematic analyses conducted for case 1.

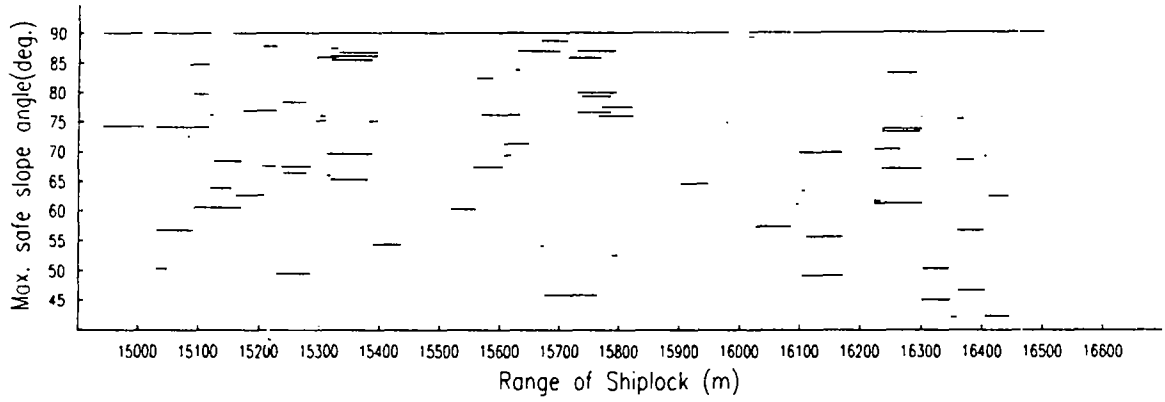

(d) Wedge Sliding - Cut Dir.=291°

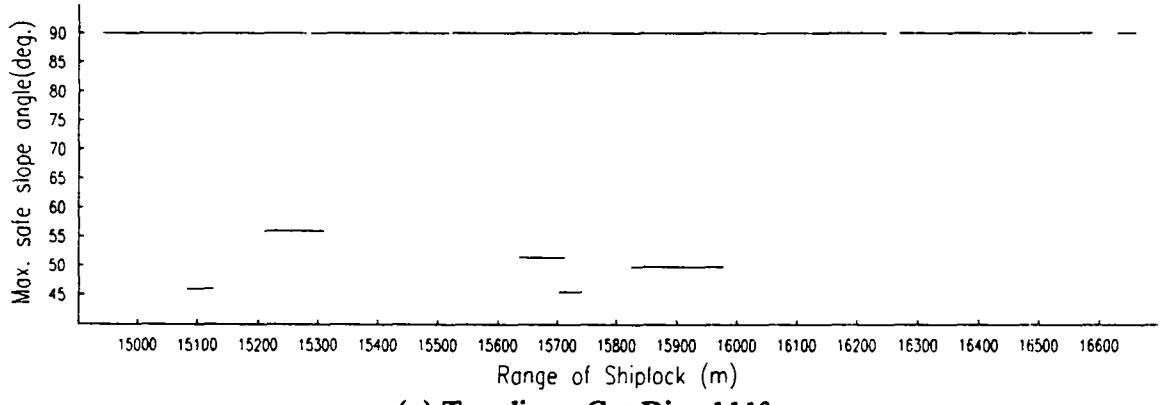

(e) Toppling - Cut Dir.=111°

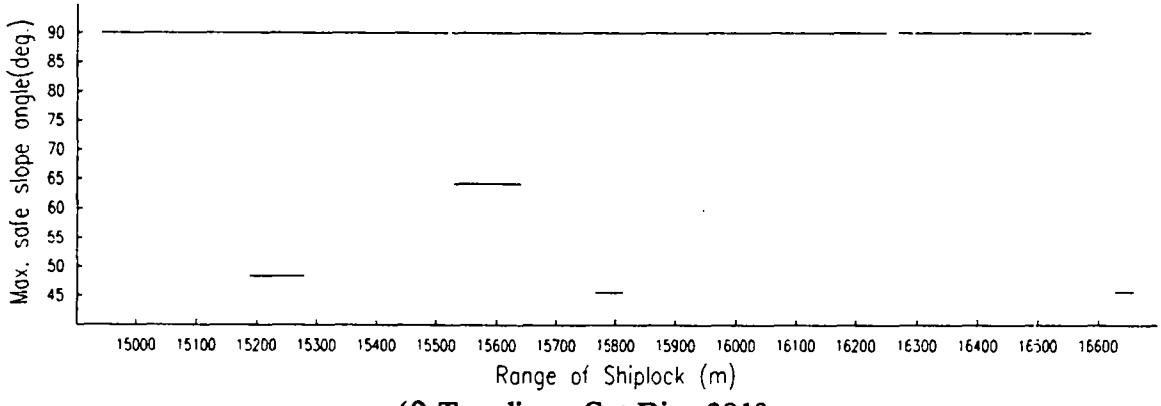

(f) Toppling - Cut Dir.=291°

Figure 10. (Continued)

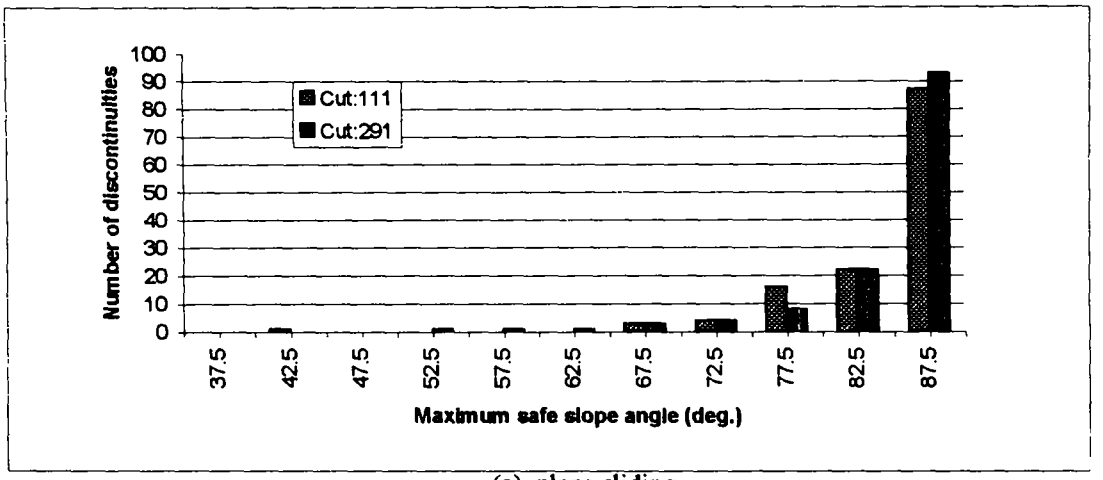

(a) plane sliding

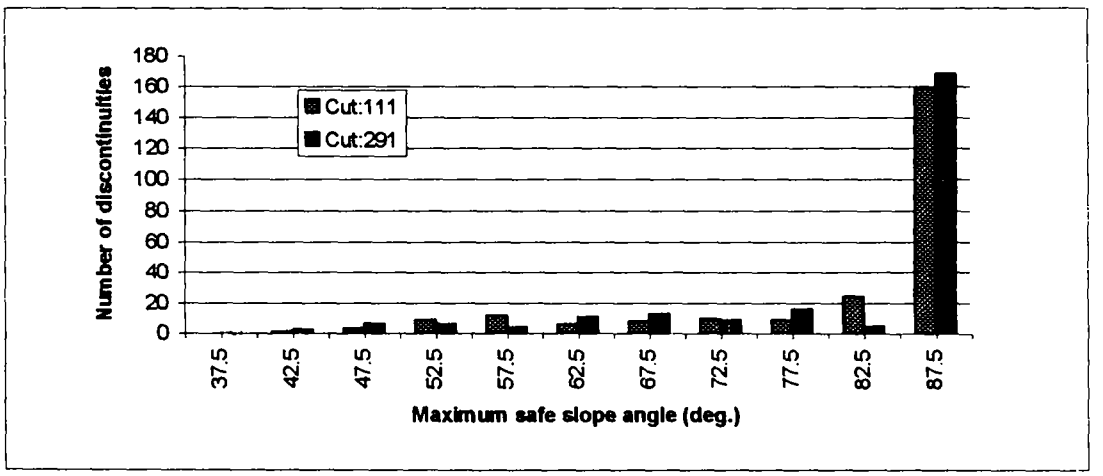

(b) wedge sliding

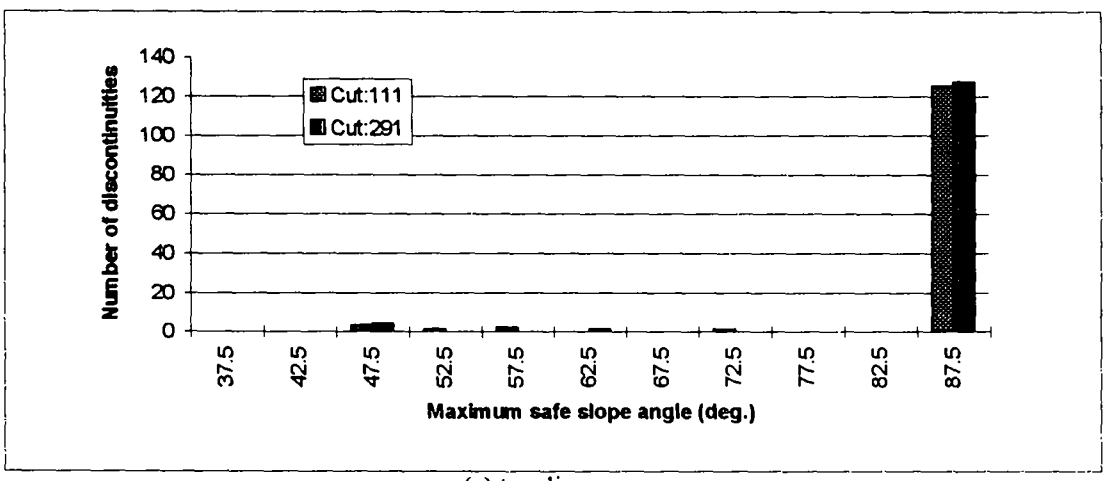

(c) toppling

Figure 11. Histograms of maximum safe slope angle for different failure modes, based on kinematic analyses conducted for case 1.

not contain a potentially unstable block were not subjected to kinematic analyses. The kinematic analyses, therefore, were performed only for 5 segments where potentially unstable blocks were found. Table 1 gives the major discontinuities and their orientations for the segments which were subjected to kinematic analyses. Note that analyses were performed separately for the SW shiplock face (strike of cut 111°) and for the NE shiplock face (strike of cut 291°). The maximum safe cut slope angles obtained for plane sliding, wedge sliding and toppling modes for these different segments are given in Table 2.

Conclusions

Kinematic analysis for plane sliding has resulted in maximum safe cut slope angles greater than 65° for most of the discontinuities. Kinematic analysis has produced maximum safe cut slope angles greater than 45° for most of the wedges. For the wedge sliding mode, only the discontinuities which are located within a 50m distance were considered in obtaining the maximum safe slope angles. Maximum safe cut slope angles greater than 85° were obtained for most of the discontinuities in the toppling case.

According to the results obtained for both cases 1 and 2, it seems that the shiplock faces in the proposed permanent shiplock region in fresh rock are more or less stable up to a cut slope of about 45°. It is important to keep in mind that this conclusion is based on the kinematic analyses performed using only the major discontinuities. In the future, kinematic analyses should be performed incorporating both major and minor discontinuities. Also, it may be worthwhile to perform kinematic analysis based on the block theory and compare the results obtained through block theory against the results obtained through the traditional kinematic analyses conducted in this study.

All the analyses conducted in this study limited the loading on the rock mass to gravitational forces only. Therefore, some kinetic analyses should be performed incorporating possible water forces, earthquake forces, etc.

Table 2 Maximum safe slope angles for different failure modes in different segments of the shiplock region resulted from case 2 analyses.

Location (m)	D_1	D_2	D_3	D_4	D_5	T_1	T_2	T_3	T_4	T_5	I_{12}	I_{13}	I_{14}	I_{15}	I_{23}	I_{24}	I_{25}	I_{34}	I_{35}	I_{45}
15150-15200	90	90	90	90	-	90	90	90	46	-	90	90	90	-	80.7	90	-	90	-	-
15550-15600	90	82.7	83.5	90	90	90	90	90	90	90	65.8	90	90	67.4	79.4	78	65.2	82.5	90	90
15750-15800	90	80.6	90	90	-	90	90	90	90	-	84.1	89.7	90	-	84.9	90	-	90	-	-
16080-16130	80.1	87	90	90	-	90	90	90	90	-	90	90	71.7	-	90	86.1	-	90	-	-
16420-16470	87.4	82.3	90	85.6	-	90	90	90	90	-	62.4	90	57.8	-	90	75.3	-	90	-	-

D_1: For Plane Sliding along Fault 1
D_2: For Plane Sliding along Fault 2
D_3: For Plane Sliding along Fault 3
D_4: For Plane Sliding along Fault 4
D_5: For Plane Sliding along Fault 5
T_1: For Toppling on Fault 1 (ϕ_j=35°)
T_2: For Toppling on Fault 2 (ϕ_j=35°)
T_3: For Toppling on Fault 3 (ϕ_j=35°)
T_4: For Toppling on Fault 4 (ϕ_j=35°)
T_5: For Toppling on Fault 5 (ϕ_j=35°)

I_{12}: For Sliding on Planes 1 and 2 Along I_{12}
I_{13}: For Sliding on Planes 1 and 3 Along I_{13}
I_{14}: For Sliding on Planes 1 and 4 Along I_{14}
I_{15}: For Sliding on Planes 1 and 5 Along I_{15}
I_{23}: For Sliding on Planes 2 and 3 Along I_{23}
I_{24}: For Sliding on Planes 2 and 4 Along I_{24}
I_{25}: For Sliding on Planes 2 and 5 Along I_{25}
I_{34}: For Sliding on Planes 3 and 4 Along I_{34}
I_{35}: For Sliding on Planes 3 and 5 Along I_{35}
I_{45}: For Sliding on Planes 4 and 5 Along I_{45}

References

Chen, D. The Geological Study of the Three Gorges Project in China. *5th Int. IAEG Congress, Buenos Aires, Argentina,* 1986, pp. 1067-1075.

Goodman, R. E. *Introduction to Rock Mechanics-2nd ed.* John wiley & sons, Inc., New York, 1989.

Ha, Q. Rock Engineering Related to the Three Gorges Project. *International Symposium on Rock Engineering Related to the Three-Gorges Project*, Yichang, China, 1993.

Kulatilake, P. H. S. W., Chen, J., Teng, J., Shufang, X. and Pan, G. Discontinuity Geometry Characterization for the Rock Mass Around a Tunnel Close to the Proposed Permanent Shiplock Area of the Three Gorges Dam Site in China. *Int. Jour. of Rock Mech. and Mining Sciences,* 1996, vol. 33, pp. 225-277.

Wang, X. Mechanism of Weathering for Crystalline Rock in the Three Gorges and Discussion of Physical and Mechanical Properties of Slightly Weathered Rock Mass. *J. Changchun Univ. of Earth Sciences,* 1986, pp. 93-100.

APPLICATION OF SOIL NAILS TO THE STABILITY OF MINE WASTE SLOPES

by

1. Clyde R. Tant
2. Eric C. Drumm and
3. Matthew Mauldon
4. Richard M. Berry

Abstract. The traditional soil nailed structure incorporates grouted or driven nails, and a wire mesh reinforced shotcrete facing to increase the stability of a slope or wall. This paper describes the construction and monitoring of a full-scale demonstration of nailing to stabilize coal mine spoil. The purpose of the investigation is to evaluate the performance of nailed slopes in mine spoil using methods proven for the stabilization of soil walls and slopes. The site in eastern Tennessee is a 12 meter high slope of dumped fill, composed of weathered shale chips, sandstone, and coal. The slope was formed by "pre-regulatory" contour surface mining operations and served as a work bench during mining. The material varies in size from silt to boulders, and has a small amount of cohesion. Portions of the mine spoil slope have experienced slope instability and erosion which have hampered subsequent reclamation activities.

Three different nail spacings and three different nail lengths were used in the design. The 12 meter high structure is instrumented to permit measurement of nail strain, and vertical inclinometer readings and survey measurements will be used for the detection of ground movement. The results of this study will aid in the development of design recommendations and construction guidelines for the application of soil nailing to stabilize mine spoil.

Key Words: Soil nailing, slope stability, contour surface mining, spoil piles

Paper presented at the 1996 Annual Meeting of the American Society for Surface Mining and Reclamation, Knoxville, Tennessee, May 1996.

1 Clyde R. Tant III is a Graduate Research Assistant, Department of Civil & Environmental Engineering, University of Tennessee, Knoxville TN 37919.

2 Eric C. Drumm is a Professor, Department of Civil & Environmental Engineering, University of Tennessee, Knoxville TN 37919.

3 Matthew Mauldon is an Associate Professor, Department of Civil & Environmental Engineering, University of Tennessee, Knoxville TN 37919.

4 Richard M. Berry is Owner and operator of Rembco Engineering, Knoxville TN.

Introduction

Throughout the Eastern Coal Province, contour surface (strip) mining has been utilized for the extraction of coal. It is not uncommon for the mine spoil and waste rock removed during mining to form unstable or marginally stable slopes. The materials forming these slopes are generally uncompacted, loose fill comprised of crushed shale and sandstone. This waste rock material forms slopes below contour surface mine high walls, or if constructed after the 1977 Surface Mining Act, may be used to reclaim high wall benches to approximate the original contour. Many of these slopes are active, with ground movement carrying trees and vegetation downslope. Throughout the Appalachian region, buildings and roadways have been constructed on or below the waste slopes. Expensive concrete retaining walls and mechanically reinforced earth structures have been constructed to stabilize the slopes and protect roads and property. In many cases the cost of remediating the slopes is not easily justified. Therefore,

practical, cost-effective, alternative construction techniques must be developed for the remediation of these slopes.

The application of earth inclusions, or soil nailing, is a proven and effective method for the stabilization of soil walls and slopes (Gässler and Gudehus, 1981; Munfakh et al., 1987; Stocker et al., 1990; Thompson and Miller, 1990; Elias & Juran, 1991). Soil nails are bars or cables, generally steel, used to reinforce a vertical or sloping face, and are usually driven or grouted into place. The construction sequence is depicted in Figure 1 (Clouterre, 1991). The nails are not tensioned and although shotcrete is often applied to

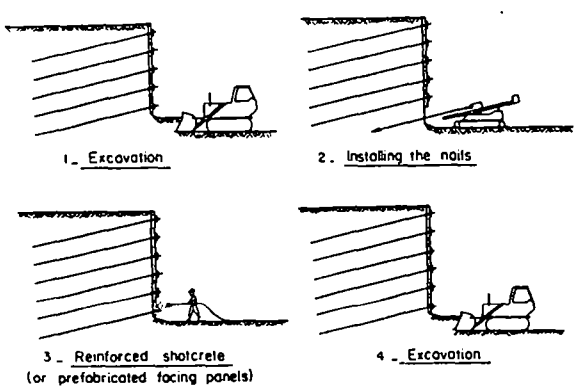

Figure 1 Schematic of soil nailed wall construction process (Clouterre, 1991)

the face, the face treatment plays a minor role in the overall stability. Construction usually occurs from the top down, with the nails gradually being loaded as the excavation progresses and the soil deforms. There are many analytical techniques used, and the construction technique is often governed by site conditions, making the technique somewhat site dependent. However, this is a major advantage of soil nailing, since the design (nail inclination, spacing, and length of nail) can easily be changed during construction based on the observed performance (Mitchell and Villet, 1987).

The purpose of this research program is to evaluate the performance and stability of nailed slopes in mine spoil using methods proven for the stabilization of soil walls and slopes. The application of these techniques to mine spoil materials has not been previously demonstrated or investigated.

Site Description

The site chosen for stabilization is in the Windrock area north of Oak Ridge, Tennessee, and is designated Buffalo Mountain on the Windrock Tennessee topographic map. The surrounding area is a combination of reclaimed sites, partially reclaimed surface mine bond forfeiture sites, and pre-1977 sites. The specific slope identified for the research is a bond forfeiture site that has experienced one or more slope failures since the mining operations were completed. The slope is comprised of loose uncompacted fill material which varies in size. It currently supports little vegetation, thus, construction and subsequent monitoring will be simplified.

The site on Buffalo Mountain is located just above 914 m (3000 ft), and is surrounded by a terrain covered with locust trees and various hardwoods. The appearance of the area changes dramatically from season to season. The site remains wet throughout the year, and from October to April, maintains a semi-frozen state. Figure 2 (Walker, 1995) shows the failure slope and remnants of the original slope, which has come to rest at the bottom of the scarp.

Figure 2 Aerial photograph of Buffalo Mountain site

Numerous contour surface mine operations were conducted in the

region. In an investigation of mine spoil stability in the eastern U.S. coal province, Swanson et al. (1983) included two nearby sites that are geologically similar to the Buffalo Mountain site. The sites (in Scott and Anderson counties) are in the Wartburg basin which is "bounded on the southeast by steeply dipping beds which form the boundary between the Cumberland Plateau and the Valley & Ridge Province"(Swanson et al., 1983). The study includes published material properties such as grain size distributions, shear strength, and compaction properties for the mine spoil. A cross section of the mined coal seams and resulting high walls in the Buffalo Mountain area is shown in Figure 3.

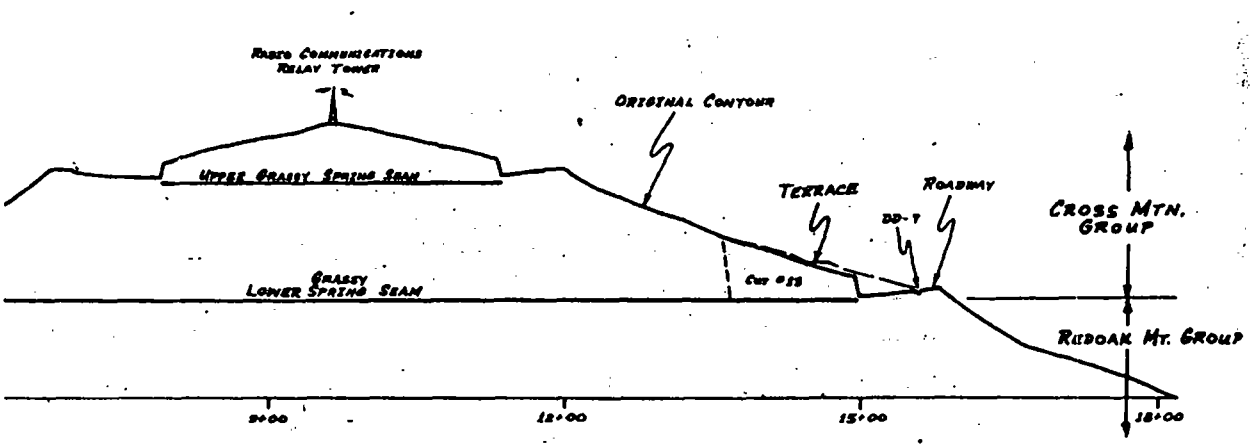

Figure 3 Geologic profile of Buffalo Mountain with strip mine highwalls

Topographic maps from pre-mining and post mining operations

An investigation of the original site terrain was conducted to determine the effects of the mining on the site topography. To investigate these effects, topographic maps from 1952 (before mining) and 1975 (after mining) were obtained. Using the coordinates supplied by the mine operators, the location of the road passing over the slope was found on the 1975 topographic map. Then the same point was located on the 1952 topographic map. Portions of the two topographic maps are shown in Figure 4 and Figure 5. A line (designated A-A) was drawn up and down slope of the road on both topographic maps. From the elevations and distances between contours along this line, a profile of the pre-mining and post mining slope was created. A comparison of the two profiles revealed that a spoil pile about 12 m (40 ft) deep was placed in the project area as shown in Figure 6.

Material Properties of Spoil

Two vertical auger borings were drilled from the road crossing the crest of the slope. From the borings, bulk samples of the spoil materials were obtained, and soil nail pullout tests were conducted. Both borings were terminated at a predetermined depth of 9 m (30 ft), which was within the mine spoil. The borings did not encounter residual soil or the mountain face. This was consistent with the profile obtained from the topographic map survey which suggested there was about 12 m (40 ft) of overburden in the slope. No ground water was encountered in either boring.

Two nail pullout tests were conducted to measure the maximum shear stress between the grout and the mine spoil. Test nails were installed in the bore holes, and after the grout cured were loaded to failure. From the pullout tests, an ultimate friction value was obtained which is an important input parameter in the design of the nailing system. The grouted portion of the nails were 200 mm (8 in) diameter and 2.4 m(8 ft) in length. Both tests yielded identical results. Table 1 lists the results of the pullout test.

Cuttings were collected from the

Figure 4 Topographic Map 1952

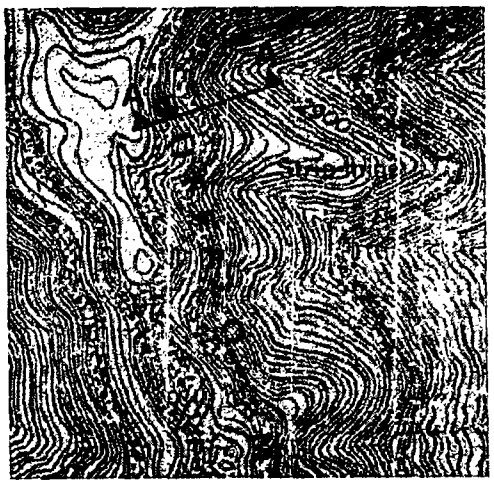

Figure 5 Topographic Map 1975

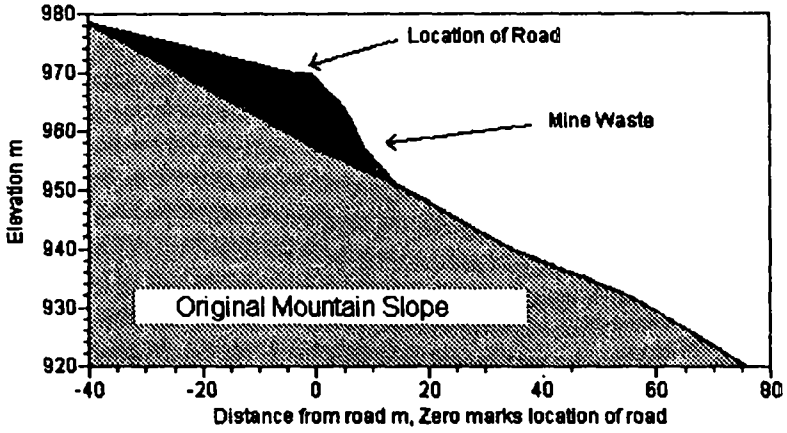

Figure 6 Profile of Buffalo Mountain in 1975 as estimated from topographic maps.

Table 1 Nail Pullout Test Results

Results of Pullout Tests Conducted 3/13/95			
Applied Load at Failure	Surface Area of Soil Nail	Displacement at Failure	Ultimate Stress in Nail
52.6 kN (11.8 kips)	1.56 m^2 (16.8 ft^2)	0.152 mm (0.006 in)	33.7 kN/m^2 (704 lb/ft^2)

boreholes and washed through a #200 sieve. A sieve analysis indicated at least 95% finer than #200. During the #200 wash, it was noticed that some of the spoil material was breaking down which suggests the material is subject to slaking. Atterberg limits were determined on a sample of mine waste from the southwest portion of the slope. The results are shown in Table 2. These results suggest that the mine spoil has a relatively narrow plasticity index, and is therefore unlikely to undergo significant volume change due to water content variation. The material would be classified as a low plasticity silt (ML) by the USCS

Table 2 Atterberg Limits of Windrock Spoil

Sample Origin	LL Liquid Limit	PL Plastic Limit	PI Plasticity Index
Windrock Spoil	31	26	5

classification system (Howard, 1984). The low PI also suggests that the nailed slope will not be subject to significant creep deformation and is well below the maximum value of 20 recommended for permanent soil nailed walls (Elias and Juran, 1991).

In-Place Testing

Due to the granular nature of the material and wide range of particle sizes, undisturbed tube samples for strength testing could not be obtained. Therefore, two in-place borehole shear tests (Lutenegger, 1987) were conducted. The tests were conducted with various consolidation times to determine effective strength parameters. The two tests yielded nearly identical results as shown in Figure 7. A best

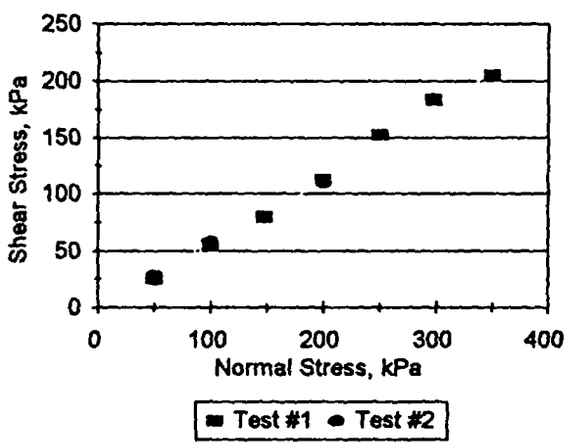

Figure 7 Results of borehole shear tets on Buffalo Mountain mine spoil

fit line through the data yields a failure envelope with a friction angle (ϕ) of about 30°. This was consistent with data reported by Swanson et al., (1983) on remolded samples of mine spoil from nearby mining operations.

Slope Stability Analysis of 1975 Slope Profile

Inspection of the slope suggests that the material possesses a small amount of cohesion that would not be measured in disturbed samples from lab and field tests. To estimate the cohesion, a profile of the slope prior to the failure (Figure 8) was estimated from the 1975 topographic map. This profile was evaluated using the STABL5 (USDOT, 1985; Carpenter, 1986) slope stability analysis program. Using the material properties in Table 3, the STABL5 program was used to back-calculate a value for the cohesion corresponding to a factor of safety, FS=1. The cohesion value was determined to be 8.6 kPa (180 psf).

Stability Analysis and Soil Nail Slope Design

Slope Stability of 1995 Slope Profile

With an estimate of the cohesion it was possible to analyze the existing slope on Buffalo Mountain. A recent slope profile obtained from an optical survey (June 1995) was used in the analysis. The water table was assumed to flow along the original topography of the mountain beneath the spoil and through the toe of the slope. This assumption was based on the absence of water at a depth of 9.0 m (30 ft) in the auger holes in the road and the observation of water at 0.3 m (1 ft) below the slope surface in a hand augered borehole at the toe of the slope. From the STABL5 analysis the factor of safety was found to be about 1.18. A factor of safety greater than one was not surprising since the slope had failed previously, as indicated by the soil mass and trees in Figure 2. Figure 9 depicts the existing slope.

Design and Analysis of Cut Slope

Since the 1995 slope profile was judged to be stable, it was decided to modify the slope to reduce the stability. By creating a steep

Table 3 Properties used in STABL5 analysis of 1975 slope profile.

Dry Unit Weight γ_d	Saturated Unit Weight γ_{sat}	Friction Angle ϕ
16.6 kN/m³ (106 lb/ft³)	18.2 kN/m³ (116 lb/ft³)	30°

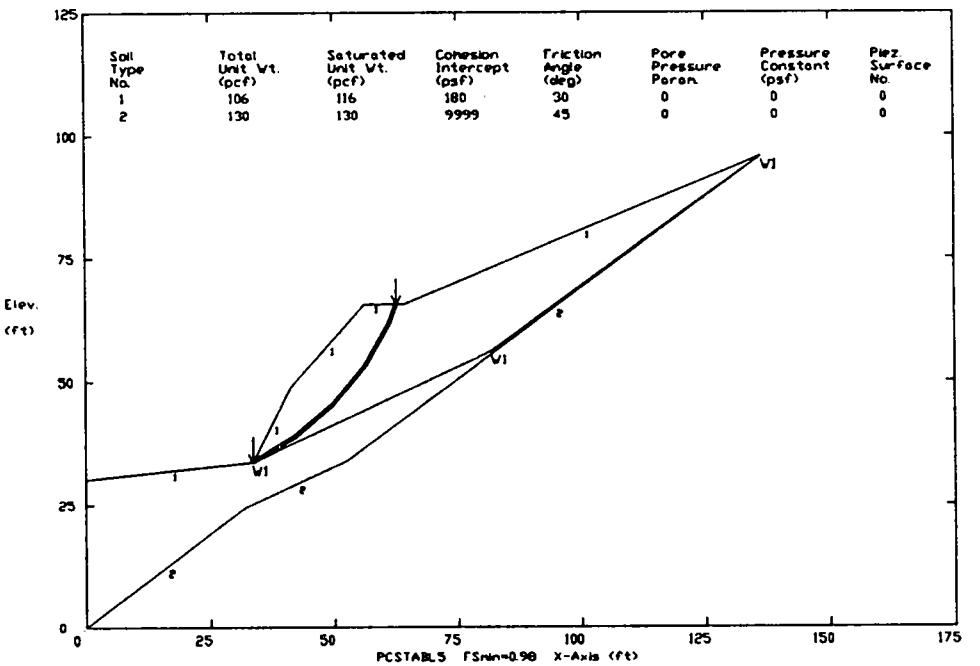

Figure 8 Stability analysis of 1975 slope profile

cut in the toe of the slope the stability was reduced. The highest unreinforced cut in the toe that can be made without instability is around 3.7 m (12 ft). Thus, it was determined that the lower 6.1 m (20 ft) of the slope would be cut as shown in Figure 10. The new slope profile consists of an upper portion 6.1 m (20 ft) high at the natural slope, and a lower portion about 6.1 m (20 ft) high cut to 15° from vertical.

To evaluate different nailing schemes, the new slope was divided into four sections. Three sections have different nailing schemes, and one control section is without nails. The upper natural slope is reinforced with four rows of nails 3.0 m (10 ft) long, spaced 1.5 m (5 ft) vertically, with horizontal spacing consistent with that of the nails below. The various nailing schemes for the lower slope are shown below in Table 4, and an elevation view of the slope is provided in Figure 11. As indicated in Table 4, the nail length as well as the horizontal spacing, S_h and vertical spacing S_v is different in all three sections.

Each section of slope was analyzed using five different methods SNAIL (Caltrans, 1992), EDINA, (Law Environmental Inc., 1991), NAIL (Geoconsult Inc., 1991), the Kinematic method (Elias and Juran, 1991) and STABL5 (USDOT, 1985; Carpenter, 1986). The material properties and resulting factors of safety for each method are listed in Table 5 and Table 6, respectively.

Different factors of safety resulted from different soil nailing analysis methods due to variations in the idealized slope. SNAIL, EDINA, FHWA, and STABL5 were all able to accommodate the natural slope above the cut slope portion in its analysis. For the NAIL program, only

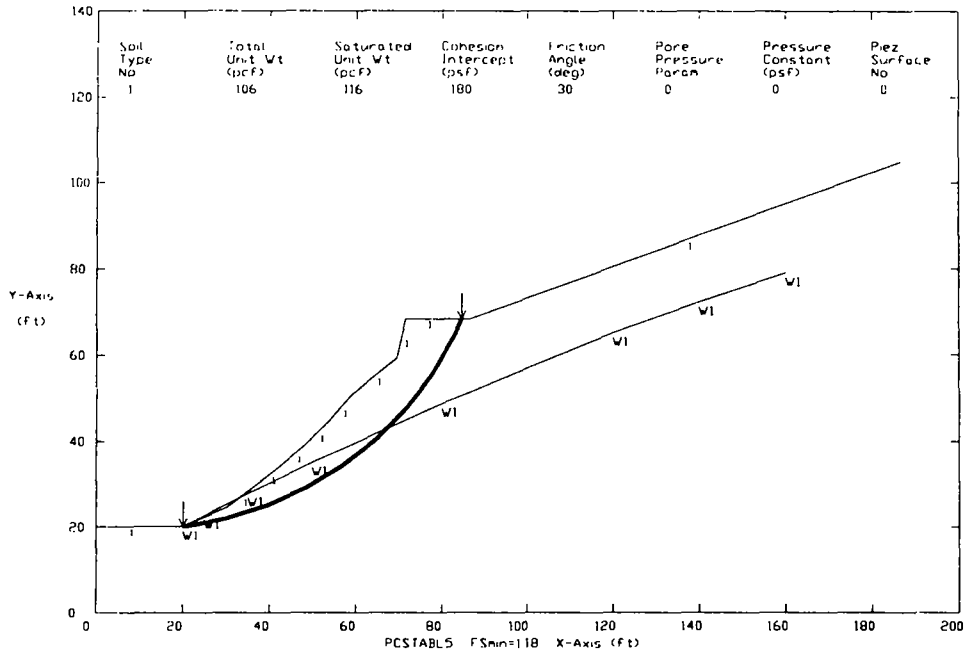

Figure 9 Stability analysis of 1995 slope

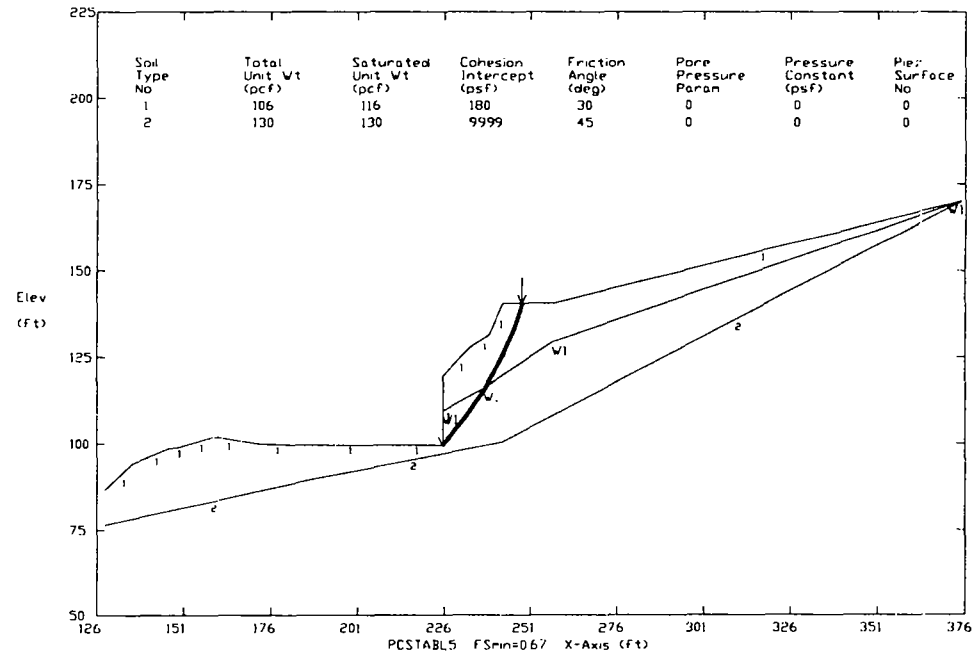

Figure 10 Profile of cut slope used in soil nailing design

Table 4 Summary of Nailing Schemes for Cut Slope

Section Row	Section 1		Section 2		Section 3	
	Sh= 1.5 m (5 ft)	Sv= 1.5 m (5 ft)	Sh= 1.8 m (6 ft)	Sv= 1.5 m (5 ft)	Sh= 1.8 m (6 ft)	Sv= 1.8 m (6 ft)
Row 1 Nail Length	6.1 m (20 ft)		4.6 m (15 ft)		4.6 m (15 ft)	
Row 2 Nail Length	6.1 m (20 ft)		4.6 m (15 ft)		3.0 m (10 ft)	
Row 3 Nail Length	6.1 m (20 ft)		4.6 m (15 ft)		3.0 m (10 ft)	
Row 4 Nail Length	6.1 m (20 ft)		3.0 m (10 ft)		3.0 m (10 ft)	

Table 5 Summary of Material Properties used for Analysis of Nailed Slope

Property	Dry Unit Weight	Saturated Unit	c	Φ
Value	16.6 kN/m³ (106 lb/ft3)	18.2 kN/m³ (116 lb/ft³)	8.6 kPa (180 lb/ft²)	30°

Table 6 Summary of Factors of Safety from Stability Analysis

Analysis Method	Program	Section 1	Section 2	Section 3	Section 4 Unreinforced
Stocker and Riedinger (1990)	SNAIL	1.31	1.12	1.06	0.9
Gässler and Gudehus (1981)	EDINA	2.39	1.03	0.83	N/A
Juran et al. (1990)	FHWA Method	1.8 6.1 m (20 ft) Nail	1.25 4.6 m (15 ft) Nail	0.5 3.0 m (10 ft) Nail	N/A
Shen et al. (1981)	NAIL	1.64	1.06	0.91	N/A
Bishop (1955)	STABL5	N/A	N/A	N/A	0.75

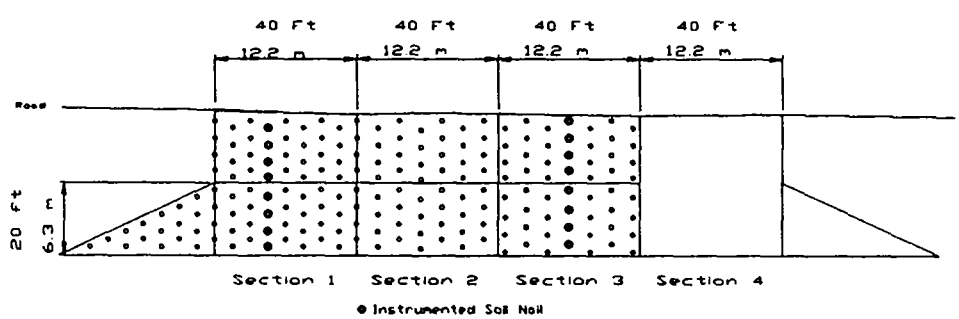

Figure 11 Elevation view of nailing and instrumentation scheme

the cut portion of the slope was analyzed, resulting in slightly elevated factors of safety. In the FHWA analysis only uniform nail length could be analyzed, therefore each section was analyzed using the uniform nail lengths included in Table 6. The results from Table 6 are compared graphically in Figure 12. The results reflect the decrease in the factor of

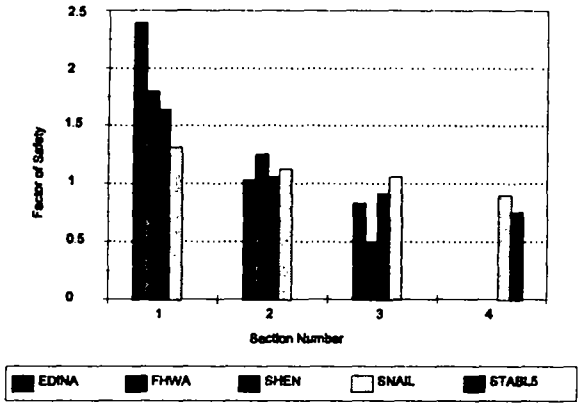

Figure 12 Comparison of factors of safety fo various analysis programs

safety from Section 1 to Section 4. The differences between the results of the analysis methods can be attributed to the difference in the idealized slopes and the manner in which the method is implemented in the computer code.

The purpose of this study is to investigate the effectiveness of soil nailing in mine spoil, therefore the four sections were designed with low factors of safety which would allow deformations of the slope and in the facing that would be observed over the life of the project.

The above analyses were conducted with an assumed water table exiting at the toe of the cut slope. This water table location assumes that the construction will draw the water table down to this elevation. To reflect the worst case water table condition, the analysis was repeated for an elevated, or short-term water table. These conditions reflect the location of the water table as it might be encountered during construction. The results of these analyses are shown in Table 7.

Like many abandoned mine land sites, Buffalo Mountain is very remote and not well suited to the application of shotcrete. Therefore, a reasonable facing which can easily be delivered and installed was selected. The facing of the slope is not the conventional shotcrete and wire mesh facing. Instead, a geosynthetic reinforced erosion blanket was installed, and held in place by steel plates attached to the nails. This should encourage the development and growth of vegetation on the slope to reduce the effects of erosion.

Instrumentation and Monitoring Program

Monitoring of the nailed slope is an important aspect of the research project. The slope deformations are monitored using vertical slope inclinometers, and surveying benchmarks. The slope inclinometers were placed in each of the four test sections and were installed to monitor the slope before, during, and after construction. To assure that the bottom of the inclinometer casing remained stationary, it was installed to a depth of 15 m (50 ft) which is 3 m (10 ft) deeper than the toe of the slope.

To record stresses in the nails, embedment strain gages, model EGP-5-350 manufactured by the Micro Measurements Group (Figure 13) were

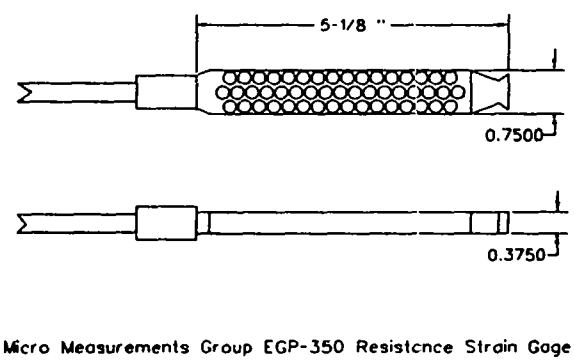

Figure 13 Embedment strain gage

utilized. In the upper natural slope, two instrumented columns of nails (Section 1 and Section 3) were instrumented as shown in Figure 11.

Table 7 Summary of Factors of Safety from Stability Analysis (Short Term Analysis)

Reference	Program	Section 1	Section 2	Section 3	Section 4 Unreinforced
Stocker and Riedinger (1990)	SNAIL	1.21	1.02	0.87	0.77
Bishop (1955)	STABL5	N/A	N/A	N/A	0.75

Both sections will each have four nails instrumented with gages, with three gages along the length of each nail. The gages are placed at 100 cm (3.2 ft), 180 cm (5.9 ft), and 230 cm (7.6 ft) along the nail relative to the facing end. For the lower portion of the slope, one column in each section will be instrumented as shown in Figure 11. The instrumentation scheme for various nail lengths is listed in Table 8. A minimum of four resistance gages will be used for a single nail.

A permanent benchmark was established to monitor deflections in the face of the slope. Reflectors will be attached along the facing, and a total station system used to monitor movements in the nails and the facing.

Construction And Monitoring

The installation of the nails was underway at the time this paper was prepared. The instruments will be monitored during construction and afterward to obtain measurements of slope deformation, nail deformation, and stress distribution in the nails. The results will be compared with those in the literature for nails in soil. Recommendations will then be made regarding the application of soil nailing to mine waste.

Acknowledgments

This project was supported by the by U.S. Bureau of Mines, Abandoned Mine Lands Program, Denver Research Center, through Contract No. 1432-J0240002. Erik Westman served as the technical contract officer. The input from Danny D. Rahnema, Douglas Siddell, and Craig Walker of the Office of Surface Mining is also appreciated.

Table 8 Summary of Strain Gage Placement for Various Nail Lengths

Nail	Gage 1*	Gage 2	Gage 3	Gage 4	Gage 5	Gage 6	Gage 7
6.1 m (20 ft)	45 cm (1.5 ft)	120 cm (4.0 ft)	195 cm (6.4 ft)	270 cm (8.9 ft)	345 cm (11.3 ft)	420 cm (13.8 ft)	495 cm (16.2 ft)
4.6 m (15 ft)	45 cm (1.5 ft)	120 cm (4.0 ft)	195 cm (6.4 ft)	270 cm (8.9 ft	345 cm (11.3 ft)	Not Used	Not Used
3.0 m (10 ft)	45 cm (1.5 ft)	120 cm (4.0 ft)	195 cm (6.4 ft)	270 cm (8.9 ft)	Not Used	Not Used	Not Used

* Location of all gages are relative to the facing end of the nail and is installed at the neutral axis to eliminate effects due to bending.

References

Bishop, A.W. (1955) "The Use of the slip circle in the stability analysis of slopes", Geotechnique, 5, No. 1, pp. 7-17.

Caltrans(1992) California Department of Transportation Division of New Technology, Materials & Research Office of Geotechnical Engineering, "SNAIL Program ver. 2.11," User's Manual. pp. 126.

Carpenter, J.R. (1985), "STABL5/PCSTABL5 User Manual, 1986, Purdue University School of Engineering, Joint Highway Research Project JHRP-86/14, West Lafayette, IN 47907

Clouterre (1991), "Soil Nailing Recommendations for Designing, Calculating, Constructing and Inspecting Earth Support Systems Using Soil Nailing," French National Research Project, Ecole Nationale des Ponts et Chaussées, Paris. English translation, July 1993, U.S. Department of Transportation, Federal Highway Administration, FHWA-SA-93-026

Elias, V. and Juran, I.(1991),"Soil Nailing for The Stabilization of Highway Slopes And Excavations," Report No. FHWA-RD-89-198, 1991, Office of Engineering & Highway Operations R&D, Federal Highway Administration, McLean, VA 22101-2296, pp 20.

Gässler, G., and Gudehus, G. (1981), Soil Nailing - some Soil Mechanical Aspects of Insitu Reinforced Earth, ICSMFE X Stockholm, 1981, Proc. Vol. 3, pp. 665-670.

Geoconsult Inc. (1991), "NAIL Program".

Howard, A.K. (1984). "The Revised ASTM Standard on the Unified Soil Classification System," Geotechnical Testing Journal, GJTODJ, Vol. 7, No.4, pp.216-222.

Juran, I., Baudrand, G., Farrag, K., Elias, V.(1990), "Kinematic Limit Analysis for Design of Soil Nailed Structures," Journal of Geotechnical Engineering, Vol. 116, No.1, pp 54-72.

Law Environmental Inc. (1991), "EDINA Program", Kennesaw, GA

Lutenegger, A.J.,(1987), "Suggested Methods for Performing the Borehole Shear Test," Geotechnical Testing Journal, GTJODL, Vol. 10, No. 1, pp. 19-25

Mitchell, J.K and Villet, W.C.B.(1987), "Reinforcement of Earth Slopes and Embankments," Report 290, National Cooperative Highway Research Program, Transportation Research Board, 323 pp.

Munfakh, G.A., Abramson, L.W., Barksdale, R.D., and Juran, I. (1987), "In-Situ Ground Reinforcement", Soil Improvement, ASCE Geotechnical Special Publication, No. 12, 1990. pp 18-35.

Shen, C.K., Bang, S., Hermann, L.R. and Romstad, J.M. (1981), "An Insitu Earth Reinforced Lateral Support System," Dept. of CE, Univ. of California at Davis, Report No. 81-03, Prepared for NSF.

Stocker, M.F., Riedinger, G., (1990). "The Bearing Behavior of Nailed Retaining Structures",Design and Performance of Earth Retaining Structures, ASCE Geotechnical Special Publication, No. 25.

Swanson, P.G, Giese, J.C. and Jones, J.S., (1983), "Surface Coal Mine Spoil Stability Study Eastern Coal Province," United States Department of the Interior Bureau of Mines, Pittsburgh Research Center,

Morgantown, West Virginia
26505, Vol I-III.

Thompson, Stephen R., Miller, R. (1990), "Design, Construction and Performance of a Soil Nailed Wall in Seattle Washington", Design and Performance of Earth Retaining Structures, ASCE Geotechnical Special Publication, Vol. 25, 1990.

USDOT (1985) U.S. Department of Transportation, Federal Highway Administration, "PC-STABL4M," Users Manual, Report No. FHWA-TS-85-229, 1985, Turner-Fairbank Highway Research Center, McLean, VA 22101-2296

Walker, Craig (1995), personal communications and aerial photography.

SESSION 5: ACID MINE DRAINAGE REMEDIATION

Page No.

Hydrologic Investigation and Remediation of a Post-Remining Acidic Seep.
William W. Aljoe, Nile A. Linberg 296

Water Quality Improvements Resulting from FBC Ash Grouting of Buried Piles of Pyritic Materials on a Surface Coal Mine.
Joseph Schueck, Mike Dimatteo, Barry Scheetz, Mike Silsbee 308

Remediation of Acid Mine Drainage within Strip Mine Spoil by Sulfate Reduction Using Waste Organic Matter.
Arthur W. Rose, Jeralee Stalker, Louise H. Michaud 321

Improving Groundwater Quality in the Backfill with Alkaline Additions.
V. Patrick Wiram, Hans E. Naumann 336

The Use of Sediment Sampling to Evaluate the Success of Hydrologic Reclamation.
Robert G. Liddle 355

Morgantown, West Virginia
26505, Vol I-III.

Thompson, Stephen R., Miller, R. (1990), "Design, Construction and Performance of a Soil Nailed Wall in Seattle Washington", Design and Performance of Earth Retaining Structures, ASCE Geotechnical Special Publication, Vol. 25, 1990.

USDOT (1985) U.S. Department of Transportation, Federal Highway Administration, "PC-STABL4M," Users Manual, Report No. FHWA-TS-85-229, 1985, Turner-Fairbank Highway Research Center, McLean, VA 22101-2296

Walker, Craig (1995), personal communications and aerial photography.